



THESIS

1



This is to certify that the

thesis entitled

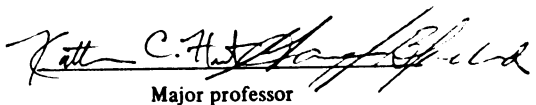
"Correlation Between Spontaneous Raman  
Intensity and Second-order Nonlinear  
Response "

presented by

Sandjaya Tjahajadiputra

has been accepted towards fulfillment  
of the requirements for

Master degree in Chemistry

  
Major professor

Date 4/7/95

**LIBRARY  
Michigan State  
University**

PLACE IN RETURN BOX to remove this checkout from your record.  
TO AVOID FINES return on or before date due.

DATE DUE	DATE DUE	DATE DUE
04/28/2015 <u>MAY 28 2005</u>		

MSU Is An Affirmative Action/Equal Opportunity Institution

c:\circldatedue.pm3-p.1

**CORRELATION BETWEEN SPONTANEOUS RAMAN INTENSITY AND  
SECOND-ORDER NONLINEAR RESPONSE**

By

**Sandjaja Tjahajadiputra**

A THESIS

Submitted to  
Michigan State University  
in partial fulfillment of the requirements  
for the degree of

**MASTER OF SCIENCE**

**Department of Chemistry**

**1995**

## ABSTRACT

### CORRELATION BETWEEN SPONTANEOUS RAMAN INTENSITY AND SECOND-ORDER NONLINEAR RESPONSE

By

Sandjaja Tjahajadiputra

A theory that relates the density  $\beta(r,r';r'',-\omega,\omega,0)$  of a second-order nonlinear response to the derivatives of the molecular polarizability with respect to normal mode coordinates has been established by Hunt *et al.* This suggests a possible correlation between vibrational Raman intensities and the nonlinear susceptibility  $\beta(-2\omega;\omega,\omega)$  responsible for frequency doubling. In this work, Raman scattering experiments have been used to test for a correlation between the spontaneous Raman scattering intensity and the second-order nonlinear susceptibility  $\beta(-2\omega;\omega,\omega)$ .

The values of the derivatives of the isotropically averaged polarizability,  $(\bar{\alpha}')$ , and the polarizability anisotropy,  $(\gamma')$ , taken with respect to normal coordinates for mono-substituted benzene molecules (chlorobenzene, bromobenzene, iodobenzene, aniline, toluene, and N-N-dimethylaniline) have been evaluated in this work and plotted versus the molecular hyperpolarizability,  $\beta$ . Correlations are found between  $(\bar{\alpha}')$  and  $(\gamma')$  and the  $\beta$  values from the literature sources. The extend of the correlation depends on the vibrational mode involved.

**To my parents, Mediarto and Sitanirawasih  
My sisters, Evy and Yenita  
My brother, Lucky  
My fiancée, Herly**

## **ACKNOWLEDGMENTS**

I would like to take this opportunity to thank Prof. Katharine Hunt and Prof. Gary Blanchard for their unending support and encouragement throughout the course of my graduate studies and during the work that led to this thesis. I am indeed grateful to them both as mentors and friends.

I would like to express my utmost appreciation to my family, especially my mom and dad, for being so supportive and understanding all this while.

Last but not least, I would also like to thank the following people, all of whom have made direct contributions, one way or another, to the enhancement of my research: Dr. Tom Carter, who made the CW laser operate perfectly, and also taught me how to use different peak fitting methods; the Hunt research group members (Ed, Xiaoping, Pao-Hua and Glenda) for their inputs toward this thesis; and the Blanchard research group members (Ying, Selezion, Patty, Jennifer, Vince, Dave and Jeff) for letting me use the laboratory equipment and chemicals needed to do this project, and for the incredible support I received from them throughout the years.

## TABLE OF CONTENTS

	<b>Page</b>
List of Tables.....	vii
List of Figures.....	viii
<b>Chapter 1: Spontaneous Vibrational Raman Scattering Theory .....</b>	<b>1</b>
1.1. Introduction to Classical Raman Scattering Theory .....	1
1.2. Raman Scattering Tensor.....	2
1.3. The Placzek Polarizability Theory .....	3
1.4. Conclusion.....	7
1.5. References .....	9
<b>Chapter 2: Relationship Between the Spontaneous Raman Intensity and the Second-order Nonlinear Response .....</b>	<b>10</b>
2.1. Introduction to Nonlinear Optical Susceptibility Theory .....	10
2.2. Static Nonlocal Polarizability Density Theory .....	14
2.3. Frequency Dependent Nonlocal Polarizability Density Theory .....	19
2.4. Relationship Between Raman Intensity and the Hyperpolarizability Density.....	25
2.5. Conclusion.....	27
2.6. References .....	28
<b>Chapter 3: Experimental Correlation Between Spontaneous Raman Scattering and the Second-order Nonlinear Response.....</b>	<b>29</b>
3.1. Overview of the Theoretical Parameters Used.....	29
3.2. Experimental Results.....	32
3.3. Conclusion.....	62
3.4. References .....	74

<b>Chapter 4: Future Work.....</b>	<b>75</b>
<b>4.1. Extension of These Experiments.....</b>	<b>75</b>
<b>4.2. Computational Calculation on the Hyperpolarizability Density         in a Non-uniform Field Environment.....</b>	<b>76</b>
<b>4.3. References.....</b>	<b>77</b>

## LIST OF TABLES

<b>Table</b>	<b>Page</b>
<b>Table 1. The Raman Intensity Obtained, Calculated Cross-section and Concentration of the Desired Molecule.....</b>	<b>37</b>
<b>Table 2. The Experimentally Obtained Intensity, Cross-sectional Area, Calculated Depolarization Ratio, (<math>\bar{\alpha}'</math>), and (<math>\gamma'</math>), of Chlorobenzene for Different Modes.....</b>	<b>44</b>
<b>Table 3. The Experimentally Obtained Intensity, Cross-sectional Area, Calculated Depolarization Ratio, (<math>\bar{\alpha}'</math>), and (<math>\gamma'</math>), of Bromobenzene for Different Modes.....</b>	<b>47</b>
<b>Table 4. The Experimentally Obtained Intensity, Cross-sectional Area, Calculated Depolarization Ratio, (<math>\bar{\alpha}'</math>), and (<math>\gamma'</math>), of Iodobenzene for Different Modes.....</b>	<b>50</b>
<b>Table 5. The Experimentally Obtained Intensity, Cross-sectional Area, Calculated Depolarization Ratio, (<math>\bar{\alpha}'</math>), and (<math>\gamma'</math>), of Toluene for Different Modes.....</b>	<b>53</b>
<b>Table 6. The Experimentally Obtained Intensity, Cross-sectional Area, Calculated Depolarization Ratio, (<math>\bar{\alpha}'</math>), and (<math>\gamma'</math>), of Aniline for Different Modes.....</b>	<b>56</b>
<b>Table 7. The Experimentally Obtained Intensity, Cross-sectional Area, Calculated Depolarization Ratio, (<math>\bar{\alpha}'</math>), and (<math>\gamma'</math>), of N-N-dimethylaniline for Different Modes.....</b>	<b>59</b>

## LIST OF FIGURES

<b>Figure</b>	<b>Page</b>
Figure 1. Schematic Diagram of the CW Argon-ion Laser.....	36
Figure 2. Raman Spectra Taken for Different Polarizations of Chlorobenzene (a) $^{\perp}I_{\perp}$ , (b) $^{\perp}I_{\parallel}$ , (c) $^{  }I_{\perp}$ , and (d) $^{  }I_{\parallel}$ .....	38
Figure 3. Raman Spectra Taken for Different Polarizations of Bromobenzene (a) $^{\perp}I_{\perp}$ , (b) $^{\perp}I_{\parallel}$ , (c) $^{  }I_{\perp}$ , and (d) $^{  }I_{\parallel}$ .....	39
Figure 4. Raman Spectra Taken for Different Polarizations of Iodobenzene (a) $^{\perp}I_{\perp}$ , (b) $^{\perp}I_{\parallel}$ , (c) $^{  }I_{\perp}$ , and (d) $^{  }I_{\parallel}$ .....	40
Figure 5. Raman Spectra Taken for Different Polarizations of Toluene (a) $^{\perp}I_{\perp}$ , (b) $^{\perp}I_{\parallel}$ , (c) $^{  }I_{\perp}$ , and (d) $^{  }I_{\parallel}$ .....	41
Figure 6. Raman Spectra Taken for Different Polarizations of Aniline (a) $^{\perp}I_{\perp}$ , (b) $^{\perp}I_{\parallel}$ , (c) $^{  }I_{\perp}$ , and (d) $^{  }I_{\parallel}$ .....	42
Figure 7. Raman Spectra Taken for Different Polarizations of N-N-dimethylaniline. (a) $^{\perp}I_{\perp}$ , (b) $^{\perp}I_{\parallel}$ , (c) $^{  }I_{\perp}$ , and (d) $^{  }I_{\parallel}$ .....	43
Figure 8. Graph of $(\bar{\alpha}')_1$ vs. $\beta$ .....	64
Figure 9. Graph of $(\bar{\alpha}')_2$ vs. $\beta$ .....	64
Figure 10. Graph of $(\bar{\alpha}')_3$ vs. $\beta$ .....	65
Figure 11. Graph of $(\bar{\alpha}')_4$ vs. $\beta$ .....	65
Figure 12. Graph of $(\bar{\alpha}')_5$ vs. $\beta$ .....	66
Figure 13. Graph of $(\gamma')_1$ vs. $\beta$ .....	66

<b>Figure 14. Graph of <math>(\gamma')</math><sub>2</sub> vs. <math>\beta</math></b> .....	67
<b>Figure 15. Graph of <math>(\gamma')</math><sub>3</sub> vs. <math>\beta</math></b> .....	67
<b>Figure 16. Graph of <math>(\gamma')</math><sub>4</sub> vs. <math>\beta</math></b> .....	68
<b>Figure 17. Graph of <math>(\gamma')</math><sub>5</sub> vs. <math>\beta</math></b> .....	68
<b>Figure 18. Graph of <math>(\bar{\alpha}')</math><sub>1</sub> vs. <math>\beta</math></b> .....	69
<b>Figure 19. Graph of <math>(\bar{\alpha}')</math><sub>2</sub> vs. <math>\beta</math></b> .....	69
<b>Figure 20. Graph of <math>(\bar{\alpha}')</math><sub>3</sub> vs. <math>\beta</math></b> .....	70
<b>Figure 21. Graph of <math>(\bar{\alpha}')</math><sub>4</sub> vs. <math>\beta</math></b> .....	70
<b>Figure 22. Graph of <math>(\bar{\alpha}')</math><sub>5</sub> vs. <math>\beta</math></b> .....	71
<b>Figure 23. Graph of <math>(\gamma')</math><sub>1</sub> vs. <math>\beta</math></b> .....	71
<b>Figure 24. Graph of <math>(\gamma')</math><sub>2</sub> vs. <math>\beta</math></b> .....	72
<b>Figure 25. Graph of <math>(\gamma')</math><sub>3</sub> vs. <math>\beta</math></b> .....	72
<b>Figure 26. Graph of <math>(\gamma')</math><sub>4</sub> vs. <math>\beta</math></b> .....	73
<b>Figure 27. Graph of <math>(\gamma')</math><sub>5</sub> vs. <math>\beta</math></b> .....	73

## **Chapter 1**

### **Spontaneous Vibrational Raman Scattering Theory**

#### **1.1. Introduction to Classical Raman Scattering Theory**

Vibrational Raman scattering is essentially a vibronic process which involves the initial, intermediate, and final vibronic states. Under special circumstances, however, it can be viewed as a purely vibrational process similar to infrared absorption. This possibility was first exploited by Placzek<sup>1</sup>.

Placzek proved that if the initial electronic state is nondegenerate and the excitation is off-resonant, the vibrational Raman intensities are given approximately by the vibrational matrix elements of the electronic polarizability. Both of these conditions are satisfied for off-resonant vibrational Raman scattering from molecules in their nondegenerate ground electronic states. The Placzek polarizability also complements the existing classical theory of vibrational Raman scattering, in which the oscillating dipole moment induced by the incident electric field light is affected by the vibrational motions, resulting in scattering with shifted frequencies.

## 1.2. Raman Scattering Tensor

The differential Raman cross-section  $\alpha_{k_s l_s k_i l_i}$  is defined by<sup>2</sup> the ratio of the number of scattered photons  $N_{k_s l_s}$  (per unit solid angle around the direction of observation  $k_s$ ) linearly polarized in the  $l_s$  direction, to the number of incident photons  $F_{k_i l_i}$  (per unit area perpendicular to the direction of the incident light beam  $k_i$ ) polarized in the  $l_i$  direction. The unit vectors  $k_i$  and  $l_i$  are perpendicular to each other and so are  $k_s$  and  $l_s$

$$N_{k_s l_s} = \alpha_{k_s l_s k_i l_i} F_{k_i l_i} \quad (1.1)$$

The cross-section for any combination of  $k_i l_i$  and  $k_s l_s$  can be expressed in terms of the nine components of a Cartesian tensor of the second rank<sup>2</sup>. This is the 'Raman scattering tensor',

$$\alpha_{k_s l_s k_i l_i} = \frac{16\pi^4}{c^4} \nu_0 (\nu_0 + \nu_m - \nu_n)^3 \left| \sum_{\rho, \sigma} (\rho \cdot l_s) (\sigma \cdot l_i) a_{\rho \sigma} \right|^2$$

$$a_{\rho \sigma} (n \leftarrow m) = \sum_{\epsilon} \left\{ \frac{\langle m | R_{\sigma} | e \rangle \langle e | R_{\rho} | n \rangle}{h(\nu_e - \nu_m - \nu_0) - i\Gamma_e} + \frac{\langle m | R_{\sigma} | e \rangle \langle e | R_{\rho} | n \rangle}{h(\nu_e - \nu_n + \nu_0) - i\Gamma_e} \right\} \quad (1.2)$$

where  $a_{\rho \sigma} (n \leftarrow m)$  is the  $\rho \sigma$  component of the Raman tensor for the transition involving the initial  $|m\rangle$ , intermediate  $|e\rangle$ , and final  $|n\rangle$  vibronic states;  $\rho$  and  $\sigma$  are unit vectors parallel to the  $\rho$  and  $\sigma$  axes;  $h\nu_m$ ,  $h\nu_e$  and  $h\nu_n$  represent the energies of  $|m\rangle$ ,  $|e\rangle$  and  $|n\rangle$  and  $h\nu_0$  is that of the exciting radiation;  $i\Gamma_e$  is the damping term introduced to avoid the divergence of Eq. (1.2) under resonant

condition. The notation  $\Sigma'$  means that  $\langle m|$  and  $\langle n|$  are excluded from the summation. The first classical derivation of  $a_{\rho\sigma}(n \leftarrow m)$  was done by Kramers and Heisenberg<sup>3</sup> and later, quantum mechanically, by Dirac<sup>4</sup>. [ Note that is the Raman scattering tensor component, whereas  $\alpha_{\rho\sigma}$  is a polarizability tensor component].

### 1.3. The Placzek Polarizability Theory

The mean square of the Raman tensor components are correlated to the Raman intensities for a randomly oriented molecular system. To perform an averaging over all orientations, it is necessary to resolve the Raman tensor  $\{a_{\rho\sigma}\}$  into three parts<sup>2</sup>,

$$\{a_{\rho\sigma}\} = \{a_{\rho\sigma}^0\} + \{a_{\rho\sigma}^s\} + \{a_{\rho\sigma}^a\} \quad (1.3)$$

where  $\{a_{\rho\sigma}^0\}$ ,  $\{a_{\rho\sigma}^s\}$ , and  $\{a_{\rho\sigma}^a\}$  are the trace, symmetric and antisymmetric parts of the Raman tensor the components of which are defined by<sup>2</sup>

$$\begin{aligned} \{a_{\rho\sigma}^0\} &= \frac{1}{3} \sum_{\rho'} a_{\rho'\rho'} \delta_{\rho\sigma} \\ \{a_{\rho\sigma}^s\} &= \frac{1}{2} (a_{\rho\sigma} + a_{\sigma\rho}) - \{a_{\rho\sigma}^0\} \\ \{a_{\rho\sigma}^a\} &= \frac{1}{2} (a_{\rho\sigma} - a_{\sigma\rho}) \end{aligned} \quad (1.4)$$

The three Placzek constants  $G^0$ ,  $G^*$  and  $G^a$  are the square moduli of  $\{a_{\rho\sigma}^0\}$ ,  $\{a_{\rho\sigma}^*\}$ , and  $\{a_{\rho\sigma}^a\}$ , and are given by<sup>1</sup>

$$\begin{aligned} G^0 &= \sum_{\rho,\sigma} |a_{\rho\sigma}^0|^2 \\ G^* &= \sum_{\rho,\sigma} |a_{\rho\sigma}^*|^2 \\ G^a &= \sum_{\rho,\sigma} |a_{\rho\sigma}^a|^2 \end{aligned} \quad (1.5)$$

which do not change in their values under rotation of the coordinates. The three Placzek invariants determine the Raman intensities from randomly oriented systems.

By use of adiabatic approximations<sup>2</sup> to the initial, intermediate, and final states, Eq. (1.2) can be expressed in a more tractable form related to molecular energy levels,

$$\begin{aligned} |m\rangle &= |g\rangle[i] \\ |n\rangle &= |g\rangle[j] \\ |e\rangle &= |e\rangle[v] \end{aligned} \quad (1.6)$$

assuming only transitions between the vibrational substates [i] and [j] of the ground electronic state |g>. [v] indicates the vibrational substate of the excited electronic state |e> acting as the intermediate state. The | ) and ( ] denote ket vectors in the electronic and vibrational spaces, respectively.

By combining Eqs. (1.2) and (1.6), an adiabatic expression for the dispersion can be obtained<sup>2</sup>,

$$a_{\rho\sigma}(j \leftarrow i) = \sum_{e \neq g} \sum_v \left\{ \frac{(i) \langle g | R_\sigma | e \rangle [v] (v) \langle e | R_\rho | g \rangle [j]}{h(\nu_{ev,gj} - \nu_0) - i\Gamma_{ev}} \right. \\ \left. + \frac{(i) \langle g | R_\rho | e \rangle [v] (v) \langle e | R_\sigma | g \rangle [j]}{h(\nu_{ev,gj} + \nu_0) - i\Gamma_{ev}} \right\} \quad (1.7)$$

where  $\hbar\nu_{ev,gj}$  and  $\hbar\nu_{ev,gj}$  are the transition energies for  $|e\rangle[v] \leftarrow |g\rangle[i]$  and  $|e\rangle[v] \leftarrow |g\rangle[j]$ .

The Placzek polarizability theory assumes the following two conditions<sup>1</sup>: First, the ground electronic state is non-degenerate and second, the energy of the exciting radiation  $\hbar\nu_0$  is so far from the resonance energy  $\hbar\nu_{ev,gj}$  that the energy difference  $h(\nu_{ev,gj} - \nu_0)$  is much larger than the vibrational energies.

The second condition leads to the following approximate relations<sup>1</sup>:

$$h(\nu_{ev,gj} + \nu_0) - i\Gamma_{ev} \approx h(\nu_{e0,g0} + \nu_0) \quad (1.8)$$

and

$$h(\nu_{ev,gj} - \nu_0) - i\Gamma_{ev} \approx h(\nu_{e0,g0} - \nu_0) \quad (1.9)$$

where  $\hbar\nu_{e0,g0}$  is the pure electronic transition energy for  $\langle e | \leftarrow \langle g |$ , and the damping constant  $\Gamma_{ev}$  is usually of the order of the vibrational energies and

hence is negligible compared with  $\hbar(\nu_{e0,g0} - \nu_0)$ . Using the completeness theorem of  $|\nu\rangle$  in the vibrational space<sup>5</sup>,

$$\sum_v |\nu\rangle (\nu) = 1 \quad (1.10)$$

the sum over  $|\nu\rangle$  in Eq. (1.7) can be left out. The new equation is given by<sup>2</sup>

$$a_{\rho\sigma}(j \leftarrow i) \equiv \langle i | \alpha_{\rho\sigma} | j \rangle$$

$$\alpha_{\rho\sigma} = \sum_{e=g} \left\{ \frac{\langle g | R_\sigma | e \rangle \langle e | R_\rho | g \rangle}{\hbar(\nu_{e0,g0} - \nu_0)} + \frac{\langle g | R_\rho | e \rangle \langle e | R_\sigma | g \rangle}{\hbar(\nu_{e0,g0} + \nu_0)} \right\} \quad (1.11)$$

where  $\alpha_{\rho\sigma}$  is the  $\rho\sigma$  component of the electronic polarizability tensor<sup>6</sup>. In Eq. (1.11), the Raman tensor component  $a_{\rho\sigma}$  is given approximately by the ij vibrational matrix element of  $\alpha_{\rho\sigma}$ , which is expressed by the adiabatic kets with the vibrational coordinates as parameters. Therefore, the Raman process involving the vibronic transitions  $|g\rangle[j] \leftarrow |e\rangle[\nu] \leftarrow |g\rangle[i]$  can be viewed as a purely vibrational transition  $[j] \leftarrow [i]$ .

For a free molecule with no external fields, there are two typical kinds of electronic degeneracy: first, the degeneracy due to the spatial symmetry of the electronic Hamiltonian, and second, the degeneracy due to time reversal symmetry<sup>7</sup>. However, degenerate states are excluded by the first assumption in Placzek theory. According to Kramers' theorem<sup>8</sup>, all electronic states of a system having an odd number of electrons must be at least be doubly degenerate

because of time reversal symmetry. Therefore, the ground electronic state  $|g\rangle$  in Eq. (1.11) must be an orbitally non-degenerate singlet state or a non-degenerate spin-orbit state of an even electron system. Time reversal symmetry implies that (1) if  $|e\rangle$  is non-degenerate,  $\langle g|R_o|e\rangle$  must be real, and (2) if  $|e\rangle$  is degenerate,  $\langle g|R_o|e\rangle$  can be made real by taking the appropriate linear combinations of the components of  $|e\rangle$ . From Eq. (1.11), the sum is taken over all degenerate components of  $|e\rangle$ , which have exactly the same energy denominators, from the earlier discussion, by taking proper linear combinations of  $\langle g|R_o|e\rangle$  and  $\langle e|R_p|g\rangle$  that are real,  $\langle g|R_o|e\rangle\langle e|R_p|g\rangle$  can be made real. Thus, the polarizability tensor  $\{\alpha_{\rho\sigma}\}$  is real and symmetric if the first assumption in Placzek theory is implied.

#### 1.4. Conclusion

Eq. (1.11) gives the formal expression in the Placzek polarizability theory. Under off-resonant conditions, the Raman tensor  $\{a_{\rho\sigma}(j \leftarrow i)\}$  is approximated by the vibrational matrix element of the electronic polarizability tensor  $\{\alpha_{\rho\sigma}\}$ , which is real and symmetric given that  $|g\rangle$  is non-degenerate. Consequently, the Raman tensor itself is real and symmetric within the framework of the

polarizability theory. This leads to the conventional polarization rule of vibrational Raman scattering, in which the values of the depolarization ratio  $\rho$  are limited to  $0 \leq \rho \leq 0.75$ .

The extension of the polarizability theory to degenerate ground electronic states has been discussed by various authors<sup>9-12</sup> and is not treated here.

## 1.5. References

1. G. Placzek, *Handbuch der Radiologie*, edited by E. Marx (Akademische Verlagsgesellschaft, Leipzig, 1934), Vol. 6, Chap. 2, p. 205.
2. H. Hamaguchi, *Advances in Infrared and Raman Spectroscopy*, edited by R. J. H. Clark and R. E. Hester, Vol. 12, Chap. 6, p. 273.
3. H. A. Kramers and W. Heisenberg, *Z. Phys.* **31**, 681 (1925).
4. P. M. Dirac, *Proc. Roy. Soc. (London)* **A114**, 710 (1927).
5. P. M. Dirac, *The Principles of Quantum Mechanics*, 4th ed., Oxford University Press, 1958.
6. H. Eyring, J. Walter, and G. E. Kimball, *Quantum Chemistry*, John Wiley and Sons, New York, 1944.
7. E. P. Wigner, *Group Theory*, Academic Press, 1959.
8. H. A. Kramers, *Koninkl. Ned. Akad. Wetenschap., Proc.* **33**, 959 (1930).
9. M. S. Child and H. C. Longuet-Higgins, *Phil. Trans. Roy. Soc. (London)* **A254**, 259 (1961).
10. M. S. Child, *Phil. Trans. Roy. Soc. (London)* **A255**, 31 (1962).
11. J. A. Koningstein, *J. Mol. Spectrosc.* **58**, 274 (1975).
12. J. A. Koningstein and T. Parameswaran, *Mol. Phys.* **32**, 1311 (1976).

## Chapter 2

### Relationship Between the Spontaneous Raman Intensity and the Second-order Nonlinear Response

#### 2.1. Introduction to Nonlinear Optical Susceptibility Theory

Nonlinear optics covers a wide range of applications -- this field deals with the nonlinear interaction of light with matter. All nonlinear optical processes involve light-induced changes of the complex dielectric response of a medium. In each nonlinear optical process, an intense electric field induces a nonlinear response in a medium, which reacts modifying the optical fields nonlinearly.

Electromagnetic phenomena are governed at the electronic level by the Maxwell's equations for the electric and magnetic fields  $\mathbf{E}(\mathbf{r}, t)$  and  $\mathbf{B}(\mathbf{r}, t)$ <sup>1</sup>,

$$\begin{aligned}\nabla \times \mathbf{E} &= -\frac{1}{c} \frac{\partial \mathbf{B}}{\partial t} \\ \nabla \times \mathbf{B} &= \frac{1}{c} \frac{\partial \mathbf{E}}{\partial t} + \frac{4\pi}{c} \mathbf{J} \\ \nabla \cdot \mathbf{E} &= 4\pi \rho \\ \nabla \cdot \mathbf{B} &= 0\end{aligned}\tag{2.1}$$

where  $\mathbf{J}(\mathbf{r}, t)$  and  $\rho(\mathbf{r}, t)$  are the current and charge densities, respectively. Charge conservation implies the equation of continuity<sup>1</sup>,

$$\nabla \cdot \mathbf{J} + \frac{\partial \rho}{\partial t} = 0.\tag{2.2}$$

One can expand  $\mathbf{J}$  and  $\rho$  into series of multipoles<sup>2</sup>,

$$\begin{aligned}\mathbf{J} &= \mathbf{J}_0 + \frac{\partial \mathbf{P}}{\partial t} + c \nabla \times \mathbf{M} + \frac{\partial}{\partial t} (\nabla \cdot \mathbf{Q}) + \dots \\ \rho &= \rho_0 - \nabla \cdot \mathbf{P} - \nabla (\nabla \cdot \mathbf{Q}) + \dots\end{aligned}\quad (2.3)$$

Here  $\mathbf{P}$ ,  $\mathbf{M}$ , and  $\mathbf{Q}$ , are the electric polarization, the magnetization, and the electric quadrupole polarization, respectively. In many cases, it is more useful to use  $\mathbf{J}$  and  $\rho$  directly as the source terms in the Maxwell's equations, or to use a generalized electric polarization,  $\mathbf{P}$ , defined by<sup>2</sup>,

$$\mathbf{J} = \mathbf{J}_0 + \frac{\partial \mathbf{P}}{\partial t} \quad (2.4)$$

where  $\mathbf{J}_0$  is the dc current density. "The generalized  $\mathbf{P}$  reduces to the electric-dipole polarization  $\mathbf{P}$ , when the magnetic dipole and higher order multipoles are neglected. The difference between  $\mathbf{P}$  and  $\mathbf{P}$  is that  $\mathbf{P}$  is a nonlocal function of the field and  $\mathbf{P}$  is local"<sup>2</sup>.

With Eqs. (2.2) and (2.4), Maxwell's equations appear in the form<sup>2</sup>,

$$\begin{aligned}\nabla \times \mathbf{E} &= -\frac{1}{c} \frac{\partial \mathbf{B}}{\partial t} \\ \nabla \times \mathbf{B} &= \frac{1}{c} \frac{\partial}{\partial t} (\mathbf{E} + 4\pi \mathbf{P}) + \frac{4\pi}{c} \mathbf{J}_0 \\ \nabla \cdot (\mathbf{E} + 4\pi \mathbf{P}) &= 0 \\ \nabla \cdot \mathbf{B} &= 0\end{aligned}\quad (2.5)$$

"where  $\mathbf{P}$  is now the time-varying source term. In general,  $\mathbf{P}$  is a function of  $\mathbf{E}$  that

describes fully the response of the medium to the field<sup>2</sup>.

The polarization  $P$  is usually a complicated nonlinear function of  $E$ . In the linear case  $P$  takes a simple linearized form given by<sup>2,2</sup>,

$$P(r,t) = \int_{-\infty}^{\infty} \chi^{(1)}(r-r',t-t') \cdot E(r',t') dr' dt' \quad (2.6)$$

where  $\chi^{(1)}$  is the linear susceptibility. The medium is assumed to be invariant, in obtaining Eq. (2.6), and if  $E$  is a monochromatic plane wave with  $E(r,t) = E(k,\omega) = \mathfrak{E}(k,\omega) \exp(i\mathbf{k} \cdot \mathbf{r} - i\omega t)$ , the Fourier transformation of (2.6) yields<sup>2</sup>,

$$\begin{aligned} P(r,t) &\rightarrow P(k,\omega) \\ &= \chi^{(1)}(k,\omega) \cdot E(k,\omega) \end{aligned} \quad (2.7)$$

with<sup>2</sup>,

$$\chi^{(1)}(k,\omega) = \int_{-\infty}^{\infty} \chi^{(1)}(r,t) \exp(-ik \cdot r + i\omega t) dr dt \quad (2.8)$$

The linear dielectric constant  $\epsilon(k,\omega)$  is related to  $\chi^{(1)}(k,\omega)$  by<sup>2</sup>,

$$\epsilon(k,\omega) = 1 + 4\pi\chi^{(1)}(k,\omega). \quad (2.9)$$

In the linear dipole approximation,  $\chi^{(1)}(k,\omega)$  is independent of  $r$ , and hence both  $\chi^{(1)}(k,\omega)$  and  $\epsilon(k,\omega)$  are independent of  $k$ . This applies for homogeneous medium, treated at the macroscopic level, but not on the microscopic level.

In the nonlinear case, when  $\mathbf{E}$  is sufficiently weak, the polarization  $\mathbf{P}$  as a function of  $\mathbf{E}$  can be expanded as power series in  $\mathbf{E}$  given by<sup>2</sup>,

$$\begin{aligned}
 \mathbf{P}(\mathbf{r}, t) = & \int_{-\infty}^{\infty} \chi^{(1)}(\mathbf{r} - \mathbf{r}', t - t') \cdot \mathbf{E}(\mathbf{r}, t') d\mathbf{r}' dt' \\
 & + \int_{-\infty}^{\infty} \chi^{(2)}(\mathbf{r} - \mathbf{r}_1, t - t_1; \mathbf{r} - \mathbf{r}_2, t - t_2) : \mathbf{E}(\mathbf{r}_1, t_1) \\
 & \quad \times \mathbf{E}(\mathbf{r}_2, t_2) d\mathbf{r}_1 dt_1 d\mathbf{r}_2 dt_2 \\
 & + \int_{-\infty}^{\infty} \chi^{(3)}(\mathbf{r} - \mathbf{r}_1, t - t_1; \mathbf{r} - \mathbf{r}_2, t - t_2; \\
 & \quad \quad \quad \mathbf{r} - \mathbf{r}_3, t - t_3) : \mathbf{E}(\mathbf{r}_1, t_1) \\
 & \quad \times \mathbf{E}(\mathbf{r}_2, t_2) \mathbf{E}(\mathbf{r}_3, t_3) d\mathbf{r}_1 dt_1 d\mathbf{r}_2 dt_2 d\mathbf{r}_3 dt_3 \\
 & + \dots
 \end{aligned} \tag{2.10}$$

where  $\chi^{(n)}$  is the  $n^{\text{th}}$ -order nonlinear susceptibility. If  $\mathbf{E}$  can be expressed as group of monochromatic plane waves  $\mathbf{E}(\mathbf{r}, t) = \sum_i \mathbf{E}(\mathbf{k}_i, \omega_i)$ , then Fourier transformation of (2.10) yields<sup>2</sup>,

$$\mathbf{P}(\mathbf{k}, \omega) = \mathbf{P}^{(1)}(\mathbf{k}, \omega) + \mathbf{P}^{(2)}(\mathbf{k}, \omega) + \mathbf{P}^{(3)}(\mathbf{k}, \omega) + \dots \tag{2.11}$$

with

$$\begin{aligned}
 \mathbf{P}^{(1)}(\mathbf{k}, \omega) &= \chi^{(1)}(\mathbf{k}, \omega) \cdot \mathbf{E}(\mathbf{k}, \omega) \\
 \mathbf{P}^{(2)}(\mathbf{k}, \omega) &= \chi^{(2)}(\mathbf{k} = \mathbf{k}_i + \mathbf{k}_j, \omega = \omega_i \pm \omega_j) : \mathbf{E}(\mathbf{k}_i, \omega_i) \mathbf{E}(\mathbf{k}_j, \omega_j) \\
 \mathbf{P}^{(3)}(\mathbf{k}, \omega) &= \chi^{(3)}(\mathbf{k} = \mathbf{k}_i + \mathbf{k}_j + \mathbf{k}_l, \omega = \omega_i \pm \omega_j \pm \omega_l) \\
 & : \mathbf{E}(\mathbf{k}_i, \omega_i) \mathbf{E}(\mathbf{k}_j, \omega_j) \mathbf{E}(\mathbf{k}_l, \omega_l)
 \end{aligned} \tag{2.12}$$

and

$$\begin{aligned} \chi^{(n)}(\mathbf{k} = \mathbf{k}_1 + \mathbf{k}_2 + \dots + \mathbf{k}_n, \omega = \omega_1 + \omega_2 + \dots + \omega_n) \\ = \int_{-\infty}^{\infty} \chi^{(n)}(\mathbf{r} - \mathbf{r}_1, t - t_1; \dots; \mathbf{r} - \mathbf{r}_n, t - t_n) \\ \times e^{-i[\mathbf{k}_1(\mathbf{r} - \mathbf{r}_1) - \omega_1(t - t_1) + \dots + \mathbf{k}_n(\mathbf{r} - \mathbf{r}_n) - \omega_n(t - t_n)]} d\mathbf{r}_1 dt_1 \dots d\mathbf{r}_n dt_n \end{aligned} \quad (2.13)$$

Similarly, in the electric dipole approximation,  $\chi^{(n)}(\mathbf{r}, t)$  is independent of  $\mathbf{r}$ , or  $\chi^{(n)}(\mathbf{k}, \omega)$  is independent of  $\mathbf{k}$ . The linear and nonlinear susceptibilities characterize the optical properties of a medium. Physically,  $\chi^{(n)}$  is related to the microscopic structure of the medium via the nonlocal polarizability density.

## 2.2. Static Nonlocal Polarizability Density Theory

Nonlocal polarizability density theory characterizes the molecular response to a local field, on a microscopic level. The nonlocal polarizability density  $\alpha(\mathbf{r}, \mathbf{r}')$  is a linear-response tensor that determines the electronic polarization induced at point  $\mathbf{r}$  in a molecule, by an external field  $\mathbf{F}^*$ , acting at point  $\mathbf{r}'$ . The electronic polarization satisfies<sup>4</sup>

$$\rho(\mathbf{r}) = -\nabla \cdot \mathbf{P}(\mathbf{r}) \quad (2.14)$$

exactly; within a molecule, there is no 'free' charge, and  $\mathbf{P}$  accounts for the higher multipole charge densities, as well as the dipole density. Then  $\mathbf{P}$

corresponds (on the microscopic level) to the generalized polarization of the previous section. This relation also holds for the polarization and charge density operators,  $\hat{P}(\mathbf{r})$  and  $\hat{\rho}(\mathbf{r})$ .

Hunt<sup>3</sup> has shown that, for a molecule perturbed by a static external field  $\mathbf{F}^*(\mathbf{r})$  the total polarization of the electronic charge distribution is related to the nonlocal polarizability density  $\alpha(\mathbf{r}, \mathbf{r}')$  and the hyperpolarizability density  $\beta(\mathbf{r}, \mathbf{r}', \mathbf{r}'')$  by

$$\begin{aligned}\mathbf{P}(\mathbf{r}) &= \mathbf{P}^{(0)}(\mathbf{r}) + \int d\mathbf{r}' \alpha(\mathbf{r}, \mathbf{r}') \cdot \mathbf{F}^*(\mathbf{r}') \\ &\quad + \frac{1}{2} \int d\mathbf{r}' d\mathbf{r}'' \beta(\mathbf{r}, \mathbf{r}', \mathbf{r}'') \mathbf{F}^*(\mathbf{r}') \mathbf{F}^*(\mathbf{r}'') + \dots \\ &= \mathbf{P}^{(0)}(\mathbf{r}) + \mathbf{P}^{\text{ind}}(\mathbf{r})\end{aligned}\quad (2.15)$$

where  $\mathbf{P}^{(0)}(\mathbf{r})$  is the static polarization at  $\mathbf{r}$  with no external perturbation.

As shown by Hunt<sup>3,5</sup>, Hunt *et al.*<sup>6</sup>, Maaskant *et al.*<sup>7</sup>, Hafkenscheid *et al.*<sup>8</sup>, and Keyes *et al.*<sup>9</sup>, the nonlocal polarizability density  $\alpha(\mathbf{r}, \mathbf{r}')$  determines the linear response to the field  $\mathbf{E}$ , and the expression for the ground-state polarizability density in terms of the sum-over-states formulation is<sup>3</sup>

$$\alpha_{\alpha\beta}(\mathbf{r}, \mathbf{r}') = \zeta_{\alpha\beta} \sum_k \frac{\langle 0 | \hat{P}_\alpha(\mathbf{r}) | k \rangle \langle k | \hat{P}_\beta(\mathbf{r}') | 0 \rangle}{(E_k - E_0)} \quad (2.16)$$

where  $\zeta_{\alpha\beta}$  symmetrizes the expression with respect to the indices of the

operators  $\hat{P}_\alpha(\mathbf{r})$  and  $\hat{P}_\beta(\mathbf{r}')$ . The prime on the summation indicates that, in summing over the states  $k$ , the ground state is omitted.

Similarly, the expression for the nonlocal hyperpolarizability density  $\beta(\mathbf{r}, \mathbf{r}', \mathbf{r}'')$  is<sup>3</sup>

$$\begin{aligned} & \beta_{\alpha\beta\gamma}(\mathbf{r}, \mathbf{r}', \mathbf{r}'') \\ &= \zeta_{\alpha\beta\gamma} \left[ \sum_{j,k} \frac{\langle 0 | \hat{P}_\alpha(\mathbf{r}) | j \rangle \langle j | \hat{P}_\beta(\mathbf{r}') | k \rangle \langle k | \hat{P}_\gamma(\mathbf{r}'') | 0 \rangle}{(E_j - E_0)(E_k - E_0)} \right. \\ & \quad \left. - \sum_k \frac{\langle 0 | \hat{P}_\alpha(\mathbf{r}) | 0 \rangle \langle 0 | \hat{P}_\beta(\mathbf{r}') | k \rangle \langle k | \hat{P}_\gamma(\mathbf{r}'') | 0 \rangle}{(E_k - E_0)^2} \right]. \end{aligned} \quad (2.17)$$

Hunt has shown that the derivatives of molecular properties with respect to the nuclear coordinates depends on nonlocal polarizability densities. When a nucleus changes its coordinate via an infinitesimal vector  $\delta\mathbf{R}'$ , there are two contributions to the change in molecular dipole moment; the first is due to the nuclear displacement and the other is due to the electronic response. This change in the nuclear coordinates also changes the electric field  $\mathbf{f}'$  at the point  $\mathbf{r}$

due to the nucleus  $I$  from  $Z^I \frac{(\mathbf{r} - \mathbf{R}^I)}{|\mathbf{r} - \mathbf{R}^I|^3}$  to<sup>11</sup>

$$\begin{aligned} f_a^I &= Z^I \frac{(\mathbf{r} - \mathbf{R}^I)_a}{|\mathbf{r} - \mathbf{R}^I|^3} + Z^I T_{\alpha\beta}(\mathbf{r} - \mathbf{R}^I) \delta\mathbf{R}_\beta^I + \dots \\ &= f_a^{I(0)} + \delta f_a^I + \dots \end{aligned} \quad (2.18)$$

where  $f_\alpha^{I(0)}$  is the field due to nucleus  $I$  in its original coordinate. The electronic charge distribution responds to the change  $\delta f_\alpha^I$  via the nonlocal polarizability density  $\alpha(r, r')$ . At lowest order, the change in the electronic polarization  $\delta P(r)$  due to the shift  $\delta R'$  is<sup>11</sup>

$$\delta P_\alpha(r) = \int d\mathbf{r}' \alpha_{\alpha\beta}(r, r') \delta f_\beta^I(r') \quad (2.19)$$

Using Eq. (2.19), one can find an expression for the change in electronic charge density  $\delta\rho(r)$  induced by the shift  $\delta R'$ ; with Eqs. (2.15), (2.16) and (2.18):<sup>11</sup>

$$\begin{aligned} \delta\rho(r) &= \int d\mathbf{r}' Z^I \nabla'_\beta \nabla'_\gamma |\mathbf{r}' - \mathbf{R}^I|^{-1} \delta R_\gamma^I \\ &\times \sum_k \frac{[\langle 0 | \hat{\rho}(r) | k \rangle \langle k | \hat{P}_\beta(r') | 0 \rangle + \langle 0 | \hat{P}_\beta(r') | k \rangle \langle k | \hat{\rho}(r) | 0 \rangle]}{(E_k - E_0)} \end{aligned} \quad (2.20)$$

where  $\nabla'_\alpha$  denotes the derivative with respect to  $r'_\alpha$ .

Equations (2.18) and (2.19) imply<sup>11</sup>

$$\delta P(r) = \int d\mathbf{r}' \alpha(r, r') \cdot Z^I T(r', \mathbf{R}^I) \cdot \delta \mathbf{R}^I \quad (2.21)$$

to the lowest order in  $\delta \mathbf{R}^I$ .

The electronic contribution to the dipole moment is the integral of  $P(r)$  over all space. Using equation (2.21) and adding the nuclear contribution gives<sup>11</sup>

$$\begin{aligned}\frac{\partial \mu_{\beta}}{\partial R_a^i} &= \frac{\partial \mu_{\beta}''}{\partial R_a^i} + \frac{\partial \mu_{\beta}'}{\partial R_a^i} \\ &= Z^i \delta_{\alpha\beta} + Z^i \int d\mathbf{r} d\mathbf{r}' \alpha_{\alpha\beta}(\mathbf{r}, \mathbf{r}') T_{\gamma\alpha}(\mathbf{r}, \mathbf{R}')\end{aligned}\quad (2.22)$$

It also should be noted that the nonlocal polarizability density has the Born symmetry<sup>10, 11</sup>

$$\alpha_{\alpha\beta}(\mathbf{r}, \mathbf{r}') = \alpha_{\beta\alpha}(\mathbf{r}', \mathbf{r}). \quad (2.23)$$

It is also possible to establish a relationship between  $\frac{\partial \alpha}{\partial \mathbf{R}^i}$  and  $\delta \mathbf{f}^i$ .

Suppose that a perturbing field  $\mathbf{F}^*(\mathbf{r})$  is applied to a molecule; then the effective nonlocal polarizability density changes from the unperturbed value  $\alpha(\mathbf{r}, \mathbf{r}')$  to<sup>11</sup>

$$\begin{aligned}\alpha_{\alpha\beta}''(\mathbf{r}, \mathbf{r}') &= \alpha_{\alpha\beta}(\mathbf{r}, \mathbf{r}') + \int d\mathbf{r}'' \beta_{\alpha\beta\gamma}(\mathbf{r}, \mathbf{r}', \mathbf{r}'') \mathbf{F}_{\gamma}^*(\mathbf{r}'') \\ &\quad + \frac{1}{2} \int d\mathbf{r}'' d\mathbf{r}''' \gamma_{\alpha\beta\gamma\delta}(\mathbf{r}, \mathbf{r}', \mathbf{r}'', \mathbf{r}''') \mathbf{F}_{\gamma}^*(\mathbf{r}'') \mathbf{F}_{\delta}^*(\mathbf{r}''') \\ &\quad + \dots\end{aligned}\quad (2.24)$$

where  $\gamma_{\alpha\beta\gamma\delta}(\mathbf{r}, \mathbf{r}', \mathbf{r}'', \mathbf{r}''')$  is the second hyperpolarizability density. An infinitesimal shift of nucleus  $I$  induces a response of the electrons to the change in the field  $\delta \mathbf{f}^i$  via the nonlocal hyperpolarizability densities<sup>11</sup> - that is, the effect due to the internal perturbation  $\delta \mathbf{f}^i$  cannot be distinguished from the effect of an external perturbation  $\mathbf{F}^*$  of the same spatial variation. Therefore,

$$\begin{aligned}\alpha_{\alpha\beta}''(\mathbf{r}, \mathbf{r}') &= \alpha_{\alpha\beta}(\mathbf{r}, \mathbf{r}') + \int d\mathbf{r}'' \beta_{\alpha\beta\gamma}(\mathbf{r}, \mathbf{r}', \mathbf{r}'') Z^i T_{\gamma\delta}(\mathbf{r}'', \mathbf{R}^i) \delta \mathbf{R}_{\delta}^i \\ &\quad + \dots\end{aligned}\quad (2.25)$$

The effective electronic polarizability is the integral of  $\alpha'_{\alpha\beta}(\mathbf{r}, \mathbf{r}')$  with respect to  $\mathbf{r}$  and  $\mathbf{r}'$  over all space. As a result, when a nuclear position in a molecule shifts infinitesimally, the change in  $\alpha(\mathbf{r}, \mathbf{r}')$  is connected to the same hyperpolarizability  $\beta_{\alpha\beta\gamma}(\mathbf{r}, \mathbf{r}', \mathbf{r}'')$  that describes the electronic charge distribution's response to external fields by<sup>11</sup>

$$\frac{\partial \alpha_{\beta\gamma}}{\partial R_\alpha^1} = \int d\mathbf{r} d\mathbf{r}' d\mathbf{r}'' \beta_{\beta\gamma\delta}(\mathbf{r}, \mathbf{r}', \mathbf{r}'') Z^1 T_{\delta\alpha}(\mathbf{r}'', \mathbf{R}^1) \quad (2.26)$$

These results show that, when the nonlocal polarizability densities are known, one can determine the dipole moment and polarizability derivatives with respect to the nuclear coordinates. A change in position, however small, of the nucleus will cause a change in the field on the electrons due to that nucleus.

Using Eq. (2.26), one can perform a direct electrostatic calculation of  $\frac{\partial \alpha_{\beta\gamma}}{\partial R_\alpha^1}$ , where all of the quantum mechanical effects are embodied in the functional forms of the polarizabilities densities.

### 2.3. Frequency Dependent Nonlocal Polarizability Density Theory

Hunt et al.<sup>12</sup> were able generalize on the static nonlocal polarizability density theory to the frequency-dependent case.

The induced electronic polarization  $\mathbf{P}^{\text{ind}}(\mathbf{r},\omega)$ , caused by a frequency-dependent external field  $\mathbf{F}(\mathbf{r},\omega)$  depends on the polarizability density  $\alpha(\mathbf{r};\mathbf{r}',\omega)$ , the hyperpolarizability density  $\beta(\mathbf{r};\mathbf{r}',\omega',\mathbf{r}'',\omega'')$ , and the other higher-order nonlinear response tensors<sup>12</sup>

$$\begin{aligned}\mathbf{P}^{\text{ind}}(\mathbf{r},\omega) &= \int d\mathbf{r}' \alpha(\mathbf{r};\mathbf{r}',\omega) \cdot \mathbf{F}(\mathbf{r}',\omega) \\ &+ \frac{1}{2} \int_{-\infty}^{\infty} d\omega' \int d\mathbf{r}' d\mathbf{r}'' \beta(\mathbf{r};\mathbf{r}',\omega-\omega',\mathbf{r}'',\omega'') : \mathbf{F}(\mathbf{r};\mathbf{r}',\omega-\omega') \mathbf{F}(\mathbf{r}'',\omega'') \\ &+ \dots\end{aligned}\quad (2.27)$$

Just as in the static case, the induced polarization,  $\mathbf{P}^{\text{ind}}(\mathbf{r},\omega)$ , is related to  $\rho^{\text{ind}}(\mathbf{r},\omega)$  by<sup>12</sup>

$$\nabla \cdot \mathbf{P}^{\text{ind}}(\mathbf{r},\omega) = -\rho^{\text{ind}}(\mathbf{r},\omega). \quad (2.28)$$

The frequency-dependent polarizability density for a molecule in the ground state is given by<sup>12</sup>

$$\begin{aligned}\alpha_{\alpha\beta}(\mathbf{r};\mathbf{r}',\omega) &= [1 + C(\omega \rightarrow -\omega)] \langle 0 | \hat{\mathbf{P}}_\alpha(\mathbf{r}) \bar{G}(\omega) \hat{\mathbf{P}}_\beta(\mathbf{r}') | 0 \rangle.\end{aligned}\quad (2.29)$$

The equation is valid when the frequency  $\omega$  is off-resonance with molecular transition frequencies,  $C(\omega \rightarrow -\omega)$  is the operator for complex conjugation and replacement of  $\omega$  by  $-\omega$ .  $\bar{G}(\omega)$  is given by<sup>12</sup>

$$\bar{G}(\omega) = (1 - \zeta_0)(H - E_0 - \hbar\omega)^{-1}(1 - \zeta_0), \quad (2.30)$$

where  $\rho_0$  is the ground-state projection operator  $|0\rangle\langle 0|$ . The nonlocal polarizability density fully determines the electronic charge redistribution linear in the perturbing field  $\mathbf{F}(\mathbf{r},\omega)$ . Integrating  $\alpha(\mathbf{r};\mathbf{r}',\omega)$  over all space with respect to  $\mathbf{r}$  and  $\mathbf{r}'$  gives the dipole polarizability  $\alpha(\omega)$ , but moments of  $\alpha(\mathbf{r};\mathbf{r}',\omega)$  also yields all of the higher multipole, linear response tensors<sup>3</sup>.

Similarly, the hyperpolarizability density  $\beta(\mathbf{r};\mathbf{r}',\omega',\mathbf{r}'',\omega'')$  gives the polarization induced at  $\mathbf{r}$  by the lowest-order nonlinear response to a field of frequency  $\omega'$  acting at point  $\mathbf{r}'$  and a field of frequency  $\omega''$  acting at  $\mathbf{r}''$ . Integrating  $\beta_{\alpha\beta\gamma}(\mathbf{r};\mathbf{r}',\omega',\mathbf{r}'',\omega'')$  with respect to  $\mathbf{r}$ ,  $\mathbf{r}'$  and  $\mathbf{r}''$  over all space yields  $\beta_{\alpha\beta\gamma}(\omega',\omega'')$ , while moment integrals of  $\beta_{\alpha\beta\gamma}(\mathbf{r};\mathbf{r}',\omega',\mathbf{r}'',\omega'')$  yield all of the third-order higher multipole susceptibilities. When  $\omega''$  is zero, the expression for the hyperpolarizability density is given by<sup>12</sup>,

$$\begin{aligned}\beta_{\alpha\beta\gamma}(\mathbf{r},\mathbf{r}',\omega',\mathbf{r}'',0) = & [1+C(\omega \rightarrow -\omega)] \{ \langle 0 | \hat{\mathbf{P}}_\alpha(\mathbf{r}) \bar{G}(\omega) [\hat{\mathbf{P}}_\gamma(\mathbf{r}'') - \mathbf{P}_\gamma^{00}(\mathbf{r}'')] \bar{G}(\omega) \hat{\mathbf{P}}_\beta(\mathbf{r}') | 0 \rangle \\ & + \langle 0 | \hat{\mathbf{P}}_\alpha(\mathbf{r}) \bar{G}(\omega) [\hat{\mathbf{P}}_\beta(\mathbf{r}') - \mathbf{P}_\beta^{00}(\mathbf{r}')] \bar{G}(0) \hat{\mathbf{P}}_\gamma(\mathbf{r}'') | 0 \rangle \\ & + \langle 0 | \hat{\mathbf{P}}_\gamma(\mathbf{r}'') \bar{G}(\omega) [\hat{\mathbf{P}}_\alpha(\mathbf{r}) - \mathbf{P}_\alpha^{00}(\mathbf{r})] \bar{G}(\omega) \hat{\mathbf{P}}_\beta(\mathbf{r}') | 0 \rangle \}. \end{aligned} \quad (2.31)$$

This equation is derived by analogy with Eq. (43.b) in Ref. 13. Also,  $\mathbf{P}_\alpha^{00}(\mathbf{r}) = \langle 0 | \hat{\mathbf{P}}_\alpha(\mathbf{r}) | 0 \rangle$ , and similarly for  $\mathbf{P}_\beta^{00}(\mathbf{r}')$  and  $\mathbf{P}_\gamma^{00}(\mathbf{r}'')$ .

Hunt *et al.*<sup>6</sup> proved that the change in polarizability density due to a change  $\delta^I$  in the internal field from nucleus I is determined by the same hyperpolarizability density  $\beta_{\alpha\beta}(\mathbf{r}; \mathbf{r}', \omega', \mathbf{r}'', \omega'')$  that fixes the response to external fields.

When Eq. (2.29) is differentiated with respect to  $R_\gamma^I$ , the result is<sup>1</sup>

$$\begin{aligned} \frac{\partial \alpha_{\alpha\beta}(\mathbf{r}; \mathbf{r}', \omega)}{\partial R_\gamma^I} = & [1 + C(\omega \rightarrow -\omega)] \left[ \left\langle \frac{\partial 0}{\partial R_\gamma^I} \left| \hat{\mathbf{P}}_\alpha(\mathbf{r}) \bar{G}(\omega) \hat{\mathbf{P}}_\beta(\mathbf{r}') \right| 0 \right\rangle \right. \\ & \left. + \left\langle 0 \left| \hat{\mathbf{P}}_\alpha(\mathbf{r}) \frac{\partial \bar{G}(\omega)}{\partial R_\gamma^I} \hat{\mathbf{P}}_\beta(\mathbf{r}') \right| 0 \right\rangle + \left\langle 0 \left| \hat{\mathbf{P}}_\alpha(\mathbf{r}) \bar{G}(\omega) \hat{\mathbf{P}}_\beta(\mathbf{r}') \right| \frac{\partial 0}{\partial R_\gamma^I} \right\rangle \right] \end{aligned} \quad (2.32)$$

The derivative of the ground state with respect to any arbitrary parameter  $\eta$  in the Hamiltonian is<sup>12</sup>

$$\left| \frac{\partial 0}{\partial \eta} \right\rangle = -\bar{G}(0) \frac{\partial H}{\partial \eta} |0\rangle \quad (2.33)$$

and the derivative of the operator  $\bar{G}(\omega)$  is given by<sup>12</sup>

$$\begin{aligned} \frac{\partial \bar{G}(\omega)}{\partial \eta} = & -\bar{G}(\omega) \frac{\partial (H - E_0)}{\partial \eta} \bar{G}(\omega) \\ & + \frac{\partial H}{\partial \eta} \bar{G}(0) \bar{G}(\omega) + \bar{G}(\omega) \bar{G}(0) \frac{\partial H}{\partial \eta} \bar{G}(0). \end{aligned} \quad (2.34)$$

To obtain the derivatives needed in Eq. (2.32), one uses Eqs. (2.33) and (2.34) with  $\eta = R_\gamma^I$ . The change in the Hamiltonian due to the shift  $\delta R_\gamma^I$  is given by

$$\frac{\partial H}{\partial R_\gamma^I} = \int d\mathbf{r} Z^I \nabla_\gamma^I |\mathbf{r} - \mathbf{R}^I|^{-1} \hat{\rho}(\mathbf{r}) \quad (2.35)$$

where  $\nabla_\gamma^I$  represents  $\frac{\partial}{\partial R_\gamma^I}$ . As in the static case,  $\frac{\partial H}{\partial R_\gamma^I}$  can be written in terms of the polarization operator  $\hat{\mathbf{P}}(\mathbf{r})$ . Using Eq. (2.15), integrating by parts with respect to  $\mathbf{r}$ , and recalling that  $\nabla_\alpha |\mathbf{r} - \mathbf{R}^I|^{-1} = -\nabla_\alpha^I |\mathbf{r} - \mathbf{R}^I|^{-1}$ , Eq. (2.35) becomes<sup>12</sup>

$$\frac{\partial H}{\partial R_\gamma^I} = - \int d\mathbf{r}'' Z^I \hat{\mathbf{P}}_\delta(\mathbf{r}'') T_{\delta\alpha}(\mathbf{r}'', \mathbf{R}^I) \quad (2.36)$$

Combining Eqs. (2.31), (2.32) - (2.34), and (2.36) the resultant equation<sup>12</sup>

$$\frac{\partial \alpha_{\beta\gamma}(\mathbf{r}; \mathbf{r}', \omega)}{\partial R_\alpha^I} = \int d\mathbf{r}'' \beta_{\beta\gamma\delta}(\mathbf{r}; \mathbf{r}', \omega, \mathbf{r}'', 0) Z^I T_{\delta\alpha}(\mathbf{r}'', \mathbf{R}^I) \quad (2.37)$$

where  $Z^I$  is the charge on nucleus  $I$  and  $T_{\delta\alpha}(\mathbf{r}'', \mathbf{R}^I)$  is the dipole propagator. When there is a shift  $\delta R^I$  in the position of nucleus  $I$  there is also a change in the nuclear Coulomb field acting on the electrons; this equation proves that the resulting change in polarizability density is determined by the same hyperpolarizability density that fixes the response to external fields.

The derivative of the polarizability  $\alpha_{\alpha\beta}(\omega)$  with respect to the normal-mode coordinate  $q_\nu$  is given by a linear combination of the derivatives in Eq. (2.37)<sup>12</sup>,

$$\frac{\partial \alpha_{\alpha\beta}(\omega)}{\partial q_v} = \sum_{I,\gamma} \frac{\partial \alpha_{\alpha\beta}(\omega)}{\partial R_\gamma^I} \frac{\partial R_\gamma^I}{\partial q_v}. \quad (2.38)$$

The Raman intensities are dependent to the matrix element  $(i|\alpha_{\rho\sigma}|j)$ .

Expanding  $\alpha_{\rho\sigma}$  as a function of the normal mode coordinates, about the equilibrium position (denoted by the superscript  $^\circ$ ),

$$\begin{aligned} \alpha_{\rho\sigma} &= \alpha_{\rho\sigma}\left(\{q_v^\circ\}\right) + \sum_v \frac{\partial \alpha_{\rho\sigma}}{\partial q_v}|_0 (q_v - q_v^\circ) \\ &\quad + \frac{1}{2} \sum_v \sum_v \frac{\partial^2 \alpha_{\rho\sigma}}{\partial q_v \partial q_v}|_0 (q_v - q_v^\circ)(q_v - q_v^\circ) \\ &\quad + \dots \end{aligned} \quad (2.39)$$

Then the matrix element becomes

$$\begin{aligned} (i|\alpha_{\rho\sigma}|j) &= \alpha_{\rho\sigma}\left(\{q_v^\circ\}\right) (i|j) + \sum_v \frac{\partial \alpha_{\rho\sigma}}{\partial q_v}|_0 (i|(q_v - q_v^\circ)|j) \\ &\quad + \frac{1}{2} \sum_v \sum_v \frac{\partial^2 \alpha_{\rho\sigma}}{\partial q_v \partial q_v}|_0 (i|(q_v - q_v^\circ)(q_v - q_v^\circ)|j) \\ &\quad + \dots \end{aligned} \quad (2.40)$$

The vibrational states are orthonormal, so for  $i \neq j$ , the first term on the right hand side vanishes. The third and higher terms correspond to vibrational overtones, which are neglected here. Then,

$$(i|\alpha_{\rho\sigma}|j) \equiv \sum_v \frac{\partial \alpha_{\rho\sigma}}{\partial q_v}|_0 (i|(q_v - q_v^\circ)|j). \quad (2.41)$$

So the electronic property that determines the intensity of vibrational Raman

scattering is the derivative of the polarizability with respect to the normal mode coordinate, within the approximation made here.

## 2.4 Relationship Between Raman Intensity and the Hyperpolarizability Density

Equation 2.37 relates  $\frac{\partial \alpha_{\beta\gamma}(r; r', \omega)}{\partial R_a^I}$  to  $\beta(r, r', \omega, r'', 0)$ . Integrating over all space with respect to  $r$  and  $r'$  yields an equation that relates  $\frac{\partial \alpha_{\beta\gamma}}{\partial R_a^I}$  to  $\beta(r, r', \omega, r'', 0)$ . It requires comparatively few assumptions; the chief requirement is that the Born-Oppenheimer approximation be valid. Connecting  $\frac{\partial \alpha_{\beta\gamma}}{\partial R_a^I}$  to the Raman intensity requires assumptions of Placzek's Theory. Subject to these conditions, the connection between Raman intensities and  $\beta(r, r', \omega, r'', 0)$  is quantum mechanically rigorous.

This suggests the possibility of a correlation between Raman intensities and the  $\beta$  hyperpolarizability tensor that gives rise to frequency doubling (as a nonlinear phenomenon). The frequency-doubling intensity depends on  $\beta(\omega, \omega)$ , which can be obtained by integrating the hyperpolarizability density

$\beta(r, r', \omega', r'', \omega)$ :

$$\beta(\omega, \omega) = \int \beta(r, r', \omega, r'', \omega) dr dr' dr''. \quad (2.42)$$

There are two differences between the integral expressions for  $\beta(\omega, \omega)$

and for  $\frac{\partial \alpha_{\beta_r}}{\partial R_a^I}$ :

1. The frequency dependence of the hyperpolarizability density

differs; for  $\beta(\omega, \omega)$  both frequencies are optical, but for  $\frac{\partial \alpha_{\beta_r}}{\partial R_a^I}$

one frequency in the hyperpolarizability density is optical while  
the other is zero.

2. The spatial integration has a dipole-propagator weighting factor

for  $\frac{\partial \alpha_{\beta_r}}{\partial R_a^I}$  while there is no weighting factor in the integral for

$\beta(\omega, \omega)$ . A molecule may have a large hyperpolarizability

density and hence a large values of  $\frac{\partial \alpha_{\beta_r}}{\partial R_a^I}$ , but a vanishing  $\beta$

due to symmetry.

For these reasons, the theory does not yield a precise relation between  
Raman intensities and  $\beta(\omega, \omega)$ ; however, it does suggest that a correlation may

exist. Experimental results and a literature survey to test for correlation are discussed in Chapter 3.

## 2.5. Conclusion

Equation (2.37) gives a new physical interpretation for integrated intensities of vibrational Raman bands, by showing that the band intensity depends on the response of the molecule to the change in the Coulomb fields of the nuclei via the  $\beta$  hyperpolarizability density. In Refs. 3 and 6, methods of finding required components of  $\alpha(r; r', 0)$  are illustrated. With sufficient information on  $\beta(r; r', \omega', r'', 0)$ , it should be possible to distinguish the regions of the electronic charge distribution that contribute the most to the vibrational Raman band intensities of isolated molecules. The dipole propagator tensors appearing in  $\frac{\partial \alpha_{\alpha\beta}(\omega)}{\partial R_\gamma^i}$  weight the regions nearest to nucleus  $i^{12}$ . This behavior supports additive approximations if  $\beta(r; r', \omega', r'', 0)$  is largest for small  $|r - r'|$  and  $|r - r''|$ .

## 2.6. References

1. V. D. Barger and M. G. Olsson, *Classical Electricity and Magnetism*, Allyn and Bacon, Massachusetts, 1987.
2. Y. R. Shen, *The Principles of Nonlinear Optics*, John Wiley & Sons, New York, 1984.
3. K. L. C. Hunt, *J. Chem. Phys.* **80**, 393 (1984).
4. J. D. Jackson, *Classical Electrodynamics*, John Wiley & Sons, New York, 1975.
5. K. L. C. Hunt, *J. Chem. Phys.* **78**, 6149 (1983).
6. K. L. C. Hunt and J. E. Bohr, *J. Chem. Phys.* **84**, 6141 (1986).
7. W. J. A. Maaskant and L. J. Oosterhoff, *Mol. Phys.* **8**, 319 (1964).
8. L. M. Hafkenscheid and J. Vlieger, *Physica* **75**, 57 (1974).
9. T. Keyes and B. M. Landanyi, *Mol. Phys.* **33**, 1271 (1977).
10. M. Born, *Optik* (Springer, Berlin, 1933), p. 406.
11. K. L. C. Hunt, , *J. Chem. Phys.* **90**, 4909 (1989).
12. K. L. C. Hunt, Y. Q. Liang, R. Nimalakirthi, and R. A. Harris, *J. Chem. Phys.* **91**, 5251 (1989).
13. B. J. Orr and J. F. Ward, *Mol. Phys.* **20**, 513 (1971).
14. A. D. Buckingham, *Proc. R. Soc. London, Ser. A* **267**, 271 (1962).
15. D. M. Bishop, *Mol. Phys.* **42**, 1219 (1981); *J. Chem. Phys.* **86**, 5613 (1987).

## Chapter 3

### Experimental Correlation Between Spontaneous Raman Scattering and the Second-order Nonlinear Response

#### 3.1. Overview of the Theoretical Parameters Used

Theories of Raman scattering with changes in the molecular vibrational state have been proposed by Behringer<sup>1</sup>, Shorygin<sup>2</sup>, Van Vleck<sup>3</sup>, Placzek<sup>4</sup>, and Albrecht<sup>5</sup>. However, the work of Peticolas *et al.*<sup>6</sup> will be used in our discussion. In spontaneous Raman scattering, an incident photon of frequency  $\omega_1$  is annihilated and the photon of frequency  $\omega_2$  and the phonon of frequency  $\omega_v$  are created.

$$\omega_v = \omega_1 - \omega_2 \quad (3.1)$$

where the transition probability of such a process can be found<sup>6,7</sup> by third -order perturbation theory.

The interaction Hamiltonian between the molecular electrons and the radiation field is given by<sup>8,9</sup>  $-\mu \cdot E$ , where  $\mu$  is the dipole moment operator and  $E$  is the electric field strength operator. The interaction between the electrons and a molecular vibration is represented by  $\left( \frac{\partial H}{\partial Q} \right)_0 Q$ , where  $H$  is the Hamiltonian of the electrons and  $Q$  is the normal coordinate of the molecular vibration. The

subscript 0 means that the derivative with respect to Q is taken at the equilibrium position of the nuclei.

The differential Raman scattering cross section per molecule per steradian in a liquid is given by<sup>10</sup>,

$$\left( \frac{d\sigma}{d\Omega} \right) = [\epsilon(\omega_2) / \epsilon(\omega_1)]^{1/2} \left( \frac{\omega_2}{c} \right)^4 \times (\hbar(\bar{\nu} + 1) / 2\omega_v) |R(-\omega_1, \omega_2, \omega_v)|^2 L \quad (3.2)$$

where  $\epsilon(\omega_1)$  and  $\epsilon(\omega_2)$  are the dielectric constants of the liquid at  $\omega_1$  and  $\omega_2$ , respectively, c is the velocity of light,  $\bar{\nu} = [\exp(\hbar\omega/kT) - 1]^{-1}$  is the average quantum number of the thermally excited vibrations of normal mode Q, L is the local field correction factor, and  $R(-\omega_1, \omega_2, \omega_v)$  is a matrix element which is given by<sup>11</sup>,

$$\begin{aligned} & R(-\omega_1, \omega_2, \omega_v) \\ &= \sum_{\alpha\beta} \left\{ \frac{\langle g' | \mathbf{e}_2 \cdot \mu | \beta' \rangle \langle \beta' | \left( \frac{\partial H}{\partial Q} \right)_0 | \alpha' \rangle \langle \alpha' | \mathbf{e}_1 \cdot \mu | g' \rangle}{(E_{\beta g}^0 - \hbar\omega_2)(E_{\alpha g}^0 - \hbar\omega_1)} \right. \\ &+ \frac{\langle g' | \mathbf{e}_1 \cdot \mu | \beta' \rangle \langle \beta' | \left( \frac{\partial H}{\partial Q} \right)_0 | \alpha' \rangle \langle \alpha' | \mathbf{e}_2 \cdot \mu | g' \rangle}{(E_{\beta g}^0 + \hbar\omega_1)(E_{\alpha g}^0 + \hbar\omega_2)} \\ & \left. + \text{four other terms} \right\} \end{aligned} \quad (3.3)$$

where  $\mathbf{e}_1$  and  $\mathbf{e}_2$  are the polarization vectors of the incident and the scattered light,  $g'$ ,  $\alpha'$ , and  $\beta'$  are the electronic wave functions of the ground and excited electronic states, and  $E_{\alpha g}^0$  and  $E_{\beta g}^0$  are the energy differences between the

excited and the ground electronic states without coupling to the molecular vibration.

When  $Q$  is a totally symmetric vibration, Kato *et al.*<sup>11</sup> assumed that the diagonal terms of  $\left(\frac{\partial H}{\partial Q}\right)_0$  should dominate over the off-diagonal terms. Since

$$\langle g | \left( \frac{\partial H}{\partial Q} \right)_0 | g \rangle = \left( \frac{\partial \langle g | H | g \rangle}{\partial Q} \right)_0 = 0 \quad (3.4)$$

the last four terms in (3.3) become zero.

Thus,  $R(-\omega_1, \omega_2, \omega_v)$  is given by<sup>11</sup>

$$\begin{aligned} R(-\omega_1, \omega_2, \omega_v) &= \sum_{\alpha} \frac{2 \left[ (E_{\alpha g}^0)^2 + \hbar \omega_1 \omega_2 \right]}{\left[ (E_{\alpha g}^0)^2 - (\hbar \omega_1)^2 \right] \left[ (E_{\alpha g}^0)^2 - (\hbar \omega_2)^2 \right]} \\ &\quad \times \langle g | e_2 \mu | \alpha \rangle \langle \alpha | \left( \frac{\partial H}{\partial Q} \right)_0 | \alpha \rangle \langle \alpha | e_1 \mu | g \rangle \end{aligned} \quad (3.5)$$

where the wavefunctions are assumed to be real.

The electrons localized on a molecule in a liquid interact with the local field which differs from the macroscopic field due to the polarization of the other molecules in the liquid. Using the results of Armstrong *et al.*<sup>12</sup> and Eckhardt *et al.*<sup>13</sup> and treating the radiation field classically gives the local field correction factor<sup>11</sup>

$$L = \{[\varepsilon(\omega_1) + 2]/3\}^2 \{[\varepsilon(\omega_2) + 2]/3\}^2 \quad (3.6)$$

Furthermore, when the incident and scattered light have the same polarization,  $R(-\omega_1, \omega_2, \omega_v)$  is equal to the squared polarizability derivative  $(\bar{\alpha}')^2 + \left(\frac{4}{45}\right)(\gamma')^2$ , where  $(\bar{\alpha}')$  and  $(\gamma')$  are the average isotropy and the anisotropy of the derived polarizability tensor with respect to the normal coordinate at the equilibrium position.

### 3.2. Experimental Results

For our experimental study, we require a group of molecules that exhibit good Raman scattering intensities. For our purposes, we chose to use a set of mono-substituted benzenes. Besides being readily available, this particular group is known to possess a strong Raman scattering character. All chemicals were purchased from Malinkrodt Chemical Company.

For a Raman scattering phenomenon, we can express the depolarization ratio in terms of the derivation of the polarizability tensor associated with the  $k^{\text{th}}$  normal mode (where  $k$  is arbitrary). The relation is<sup>14</sup>,

$$\rho_n = \frac{6\gamma'^2}{45(\bar{\alpha}')^2 + 7\gamma'^2}. \quad (3.7)$$

The matrix element<sup>2</sup> is

$$|R|^2 = (\bar{\alpha}')^2 + \left(\frac{4}{45}\right)(\gamma')^2. \quad (3.8)$$

Combining Eqs. (3.7) and (3.8), we obtain

$$|R|^2 = \frac{(6-3\rho_n)}{(6-7\rho_n)} (\bar{\alpha}')^2 \quad (3.9)$$

By use of Eq. (3.9), tedious mathematical expressions otherwise needed to evaluate the matrix element can be avoided. Also, by combining equations (3.2), (3.6), and (3.9), assuming that the dielectric constants are approximately equal ( $\epsilon_1 \approx \epsilon_2$ ) and also directly proportional to the square of the refractive index of the molecule, we obtain

$$\begin{aligned} (\bar{\alpha}')^2 &= \left(1 - \frac{4}{\left(\frac{6}{\rho_n} - 3\right)}\right) \left(\frac{81}{(n^2 + 2)^2}\right) \left(\frac{c}{\omega_2}\right)^4 \\ &\times \left(\frac{2\omega_v}{\hbar(\bar{\nu}+1)}\right) \left(\frac{\partial\sigma}{\partial\Omega}\right). \end{aligned} \quad (3.10)$$

Similarly,

$$\begin{aligned} (\gamma')^2 &= \left(\frac{45}{6-3\rho_n}\right) \left(\frac{81}{(n^2 + 2)^2}\right) \left(\frac{c}{\omega_2}\right)^4 \\ &\times \left(\frac{2\omega_v}{\hbar(\bar{\nu}+1)}\right) \left(\frac{\partial\sigma}{\partial\Omega}\right). \end{aligned} \quad (3.11)$$

To obtain the values of  $(\bar{\alpha}')^2$  and  $(\gamma')^2$ , we need to find the values of the depolarization ratio and the scattering cross-section.

The values of the depolarization ratio can be obtained experimentally, via<sup>14</sup>

$$\rho_n = \frac{^0 I_{\perp}(\pi/2) + ^1 I_{\parallel}(\pi/2)}{^1 I_{\perp}(\pi/2) + ^1 I_{\parallel}(\pi/2)} \quad (3.12)$$

where  $\perp$  is an abbreviation for perpendicular and  $I$  is an abbreviation for parallel.

$^0 I_{\parallel}(\pi/2)$  denotes the radiant intensity of scattered radiation plane-polarized parallel to the scattering plane and propagating along a direction in the scattering plane making an angle  $(\pi/2)$  to the direction of the incident radiation plane-polarized parallel to the scattering plane.

In our experimental study, we used a CW Argon ion laser, with a 488 nm excitation wavelength and the schematic layout shown in Figure 1. A 1-cm pathlength cuvette was used as the sample holder.

The first experiments that were carried out yielded the average cross-sectional area for the mono-substituted benzene molecules (chlorobenzene, bromobenzene, iodobenzene, toluene, aniline and N-N-dimethylaniline) using benzene as the standard. Table 1 summarizes the values obtained and calculated, for the respective normal mode, from these experiments.

Figures 2 to 7 show the various bands intensities as functions of the polarization of the radiation field. In order to calculate the intensities, a peak fitting module program, called Origin, was used. The Origin peak fitting module is primarily designed to analyze data with many peaks. The kernel of the module is the Levenberg-Marquardt non-linear least-squares curve fitter, the Lorentzian fitting function had been used<sup>15</sup>,

$$y = \frac{2A}{\pi} \cdot \frac{\omega}{4(x - xc)^2 + \omega^2} \quad (3.13)$$

where  $xc$  is the center of the peak,  $A$  is the area and  $\omega$  is the full width at half maximum.

After determining the values of the intensities, the rest of the calculations were done using the equations given above to obtain the values of  $(\bar{\alpha}')^2$  and  $(\gamma')^2$ , and thus  $(\bar{\alpha}')$  and  $(\gamma')$ . These values are tabulated in Tables 2 to 7. There are differences in the values of the intensities with different polarizations because laser power used is different from day to day.

In the case of N-N-dimethylaniline, there are only four possible modes that can be observed because N-N-dimethylaniline fluoresces after sometime during the experiment; and hence, peaks that are located in the lower Raman shift frequency (less than  $400 \text{ cm}^{-1}$ ) are harder to determine due to the fluorescence effects.

Figure 1.

Schematic diagram of the CW Argon ion laser

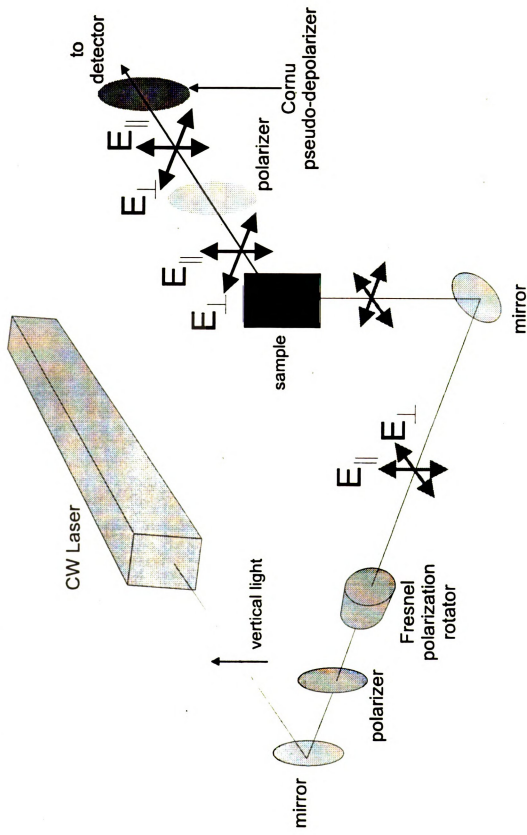




**Table 1.** The Raman intensity obtained, calculated cross-section and concentration of the desired molecule.

Molecule	Raman Intensity			Cross-section ( $\times 10^{-29}$ cm <sup>2</sup> .molecule <sup>-1</sup> .Sr <sup>-1</sup> )	Average cross-section ( $\times 10^{-29}$ cm <sup>2</sup> .molecule <sup>-1</sup> .Sr <sup>-1</sup> )	Concentration (M)
	expt.1	expt.2	expt.3	expt.1	expt.2	expt.3
C <sub>6</sub> H <sub>6</sub>	761136	937579	788340	3.250 <sup>12</sup>	3.250	3.250
C <sub>6</sub> H <sub>5</sub> Cl	303205	379522	323450	1.476	1.503	1.523
C <sub>6</sub> H <sub>5</sub> Br	334433	376796	318214	1.687	1.543	1.550
C <sub>6</sub> H <sub>5</sub> I	353970	205387	387525	1.890	0.8902	1.998
C <sub>6</sub> H <sub>5</sub> CH <sub>3</sub>	277449	359331	306165	1.413	1.486	1.506
C <sub>6</sub> H <sub>5</sub> NH <sub>2</sub>	625307	681703	546540	2.044	1.932	2.041
C <sub>6</sub> H <sub>5</sub> N(CH <sub>3</sub> ) <sub>2</sub>	244590	549573	NA	0.6671	1.254	NA
						0.9605
						7.887

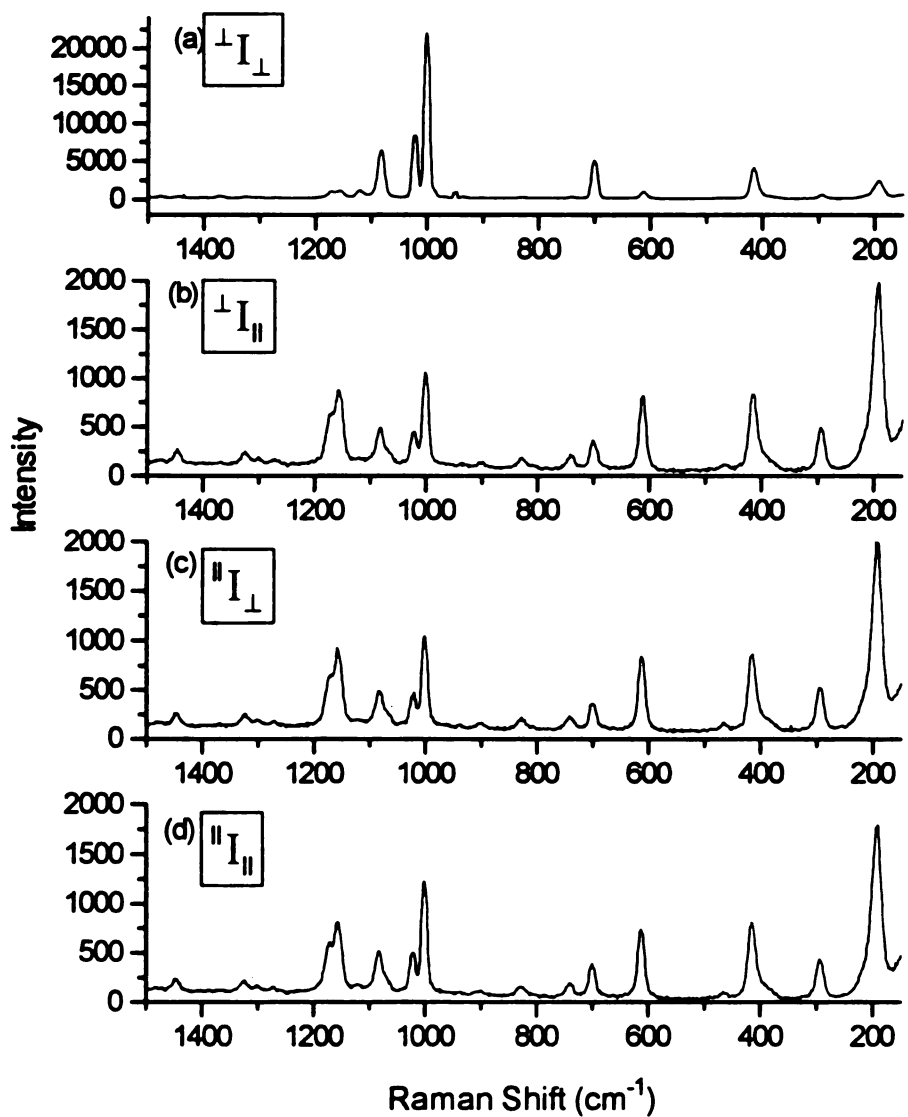


**Figure 2** Raman spectra taken for different polarizations of chlorobenzene.  
(a)  $\perp I_{\perp}$ , (b)  $\perp I_{\parallel}$ , (c)  $\parallel I_{\perp}$ , (d)  $\parallel I_{\parallel}$ .

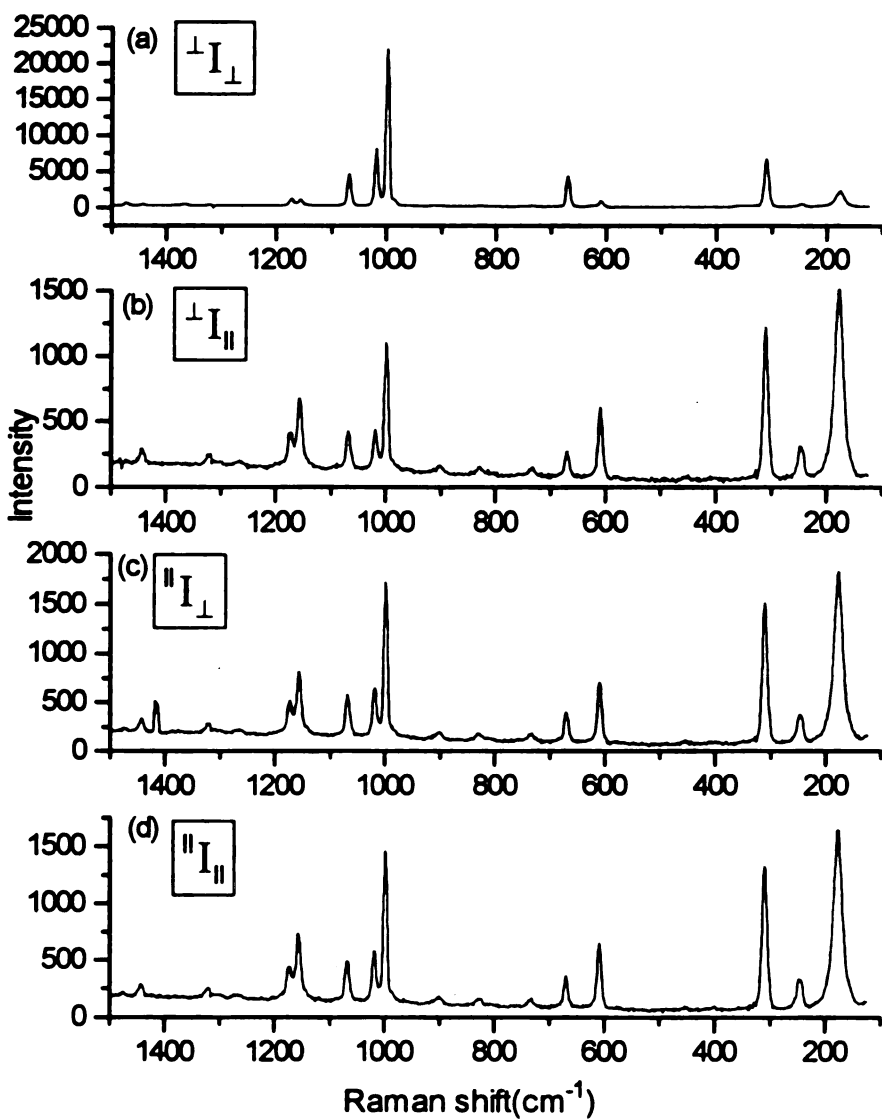
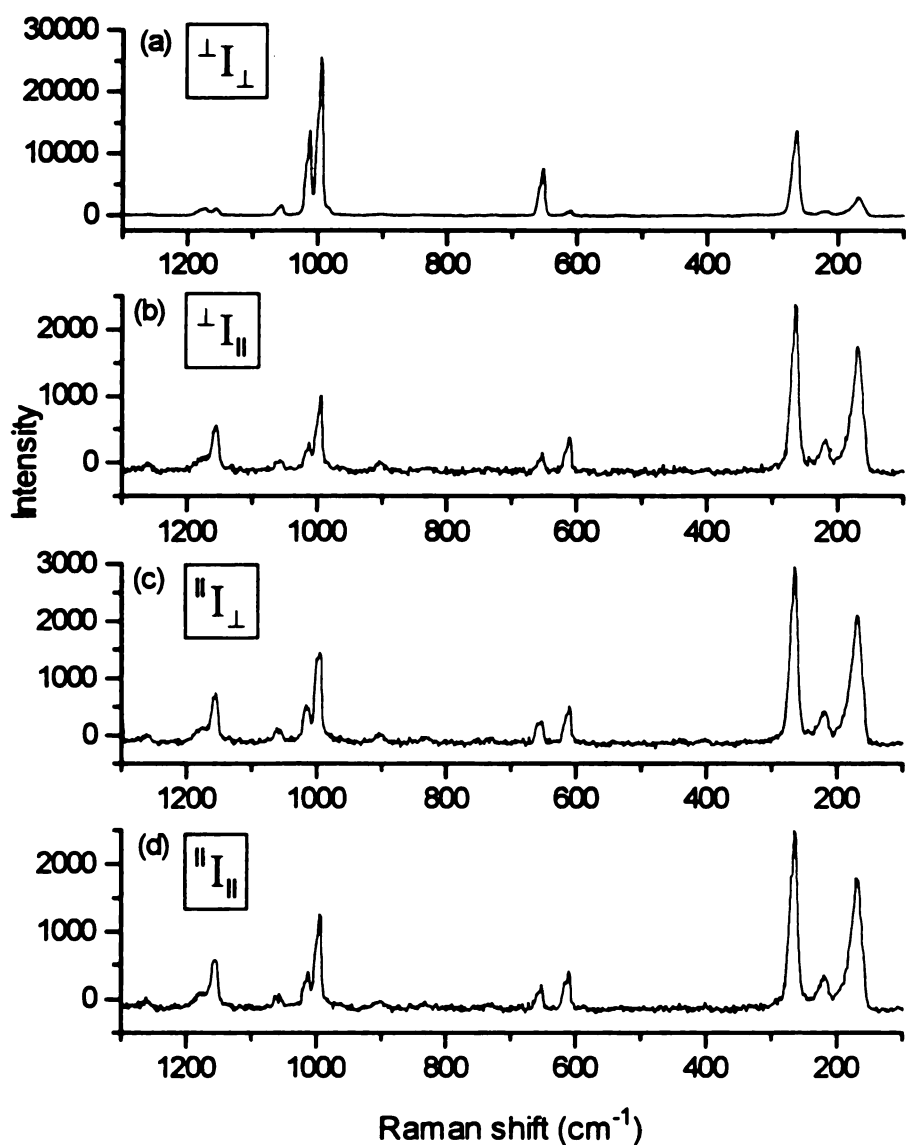
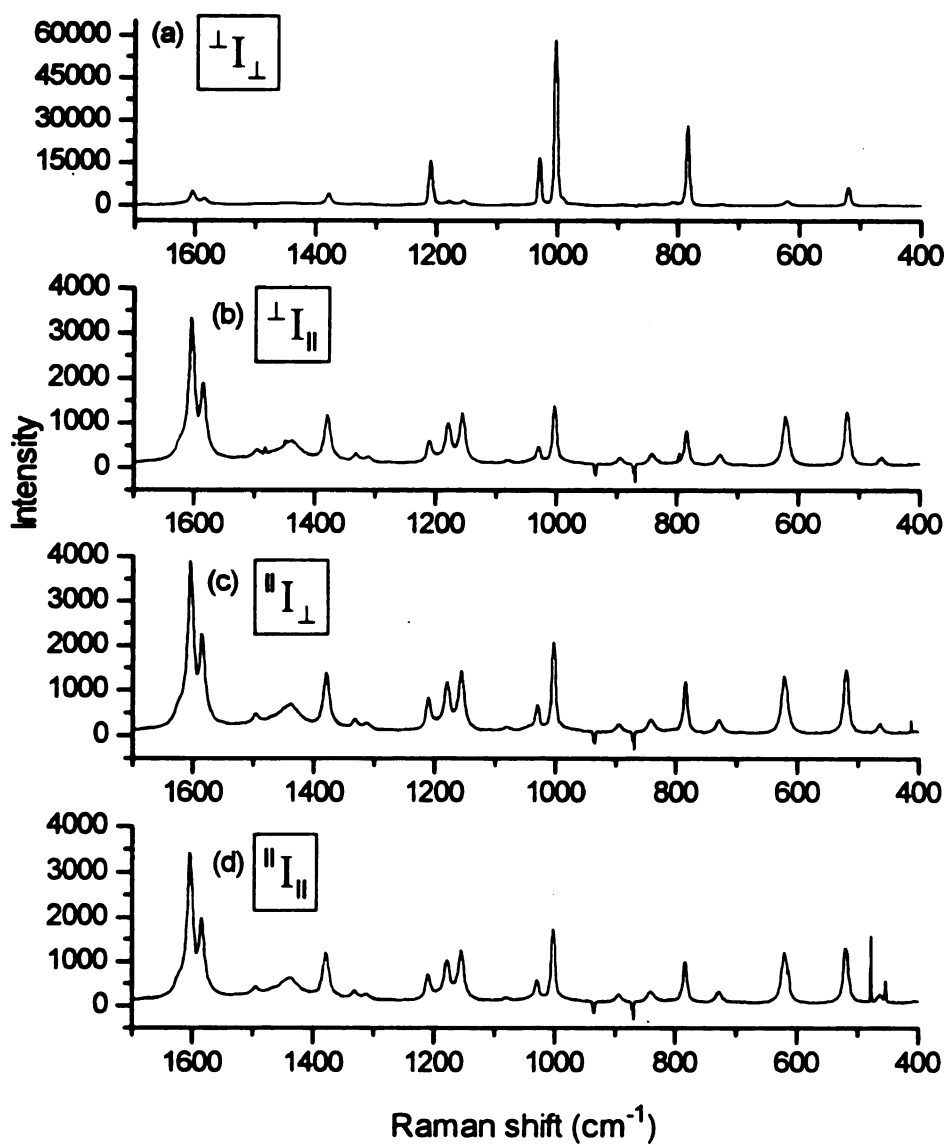


Figure 3. Raman spectra taken for different polarizations of bromobenzene.  
(a)  $\perp I_{\perp}$ , (b)  $\perp I_{\parallel}$ , (c)  $\parallel I_{\perp}$ , (d)  $\parallel I_{\parallel}$ .



**Figure 4.** Raman spectra taken for different polarizations of iodobenzene.  
(a)  $\perp I_{\perp}$ , (b)  $\perp I_{\parallel}$ , (c)  $\parallel I_{\perp}$ , (d)  $\parallel I_{\parallel}$ .



**Figure 5.** Raman spectra taken for different polarizations of toluene.  
 (a)  $\perp I_{\perp}$ , (b)  $\perp I_{\parallel}$ , (c)  $\parallel I_{\perp}$ , (d)  $\parallel I_{\parallel}$

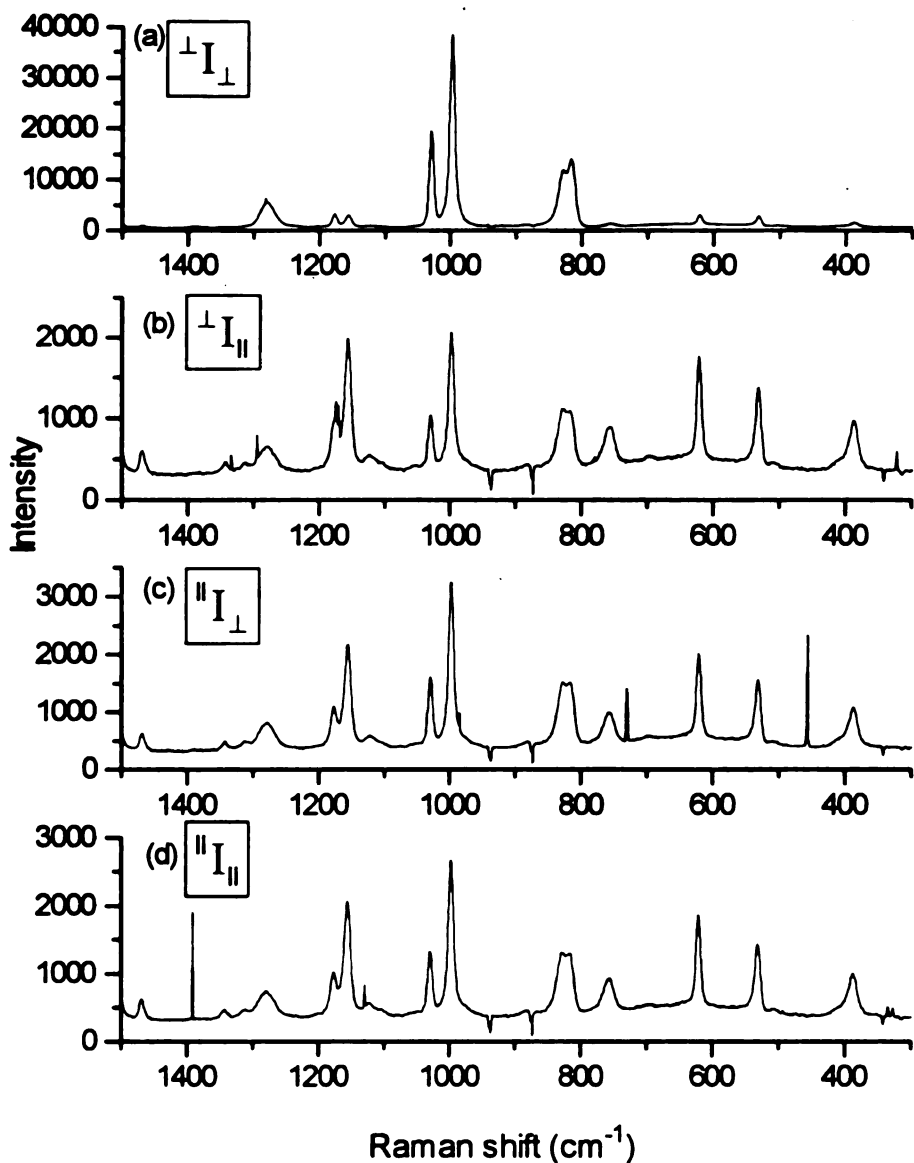


**Figure 6.** Raman spectra taken for different polarizations of aniline.  
(a)  $\perp I_{\perp}$ , (b)  $\perp I_{\parallel}$ , (c)  $\parallel I_{\perp}$ , (d)  $\parallel I_{\parallel}$ .

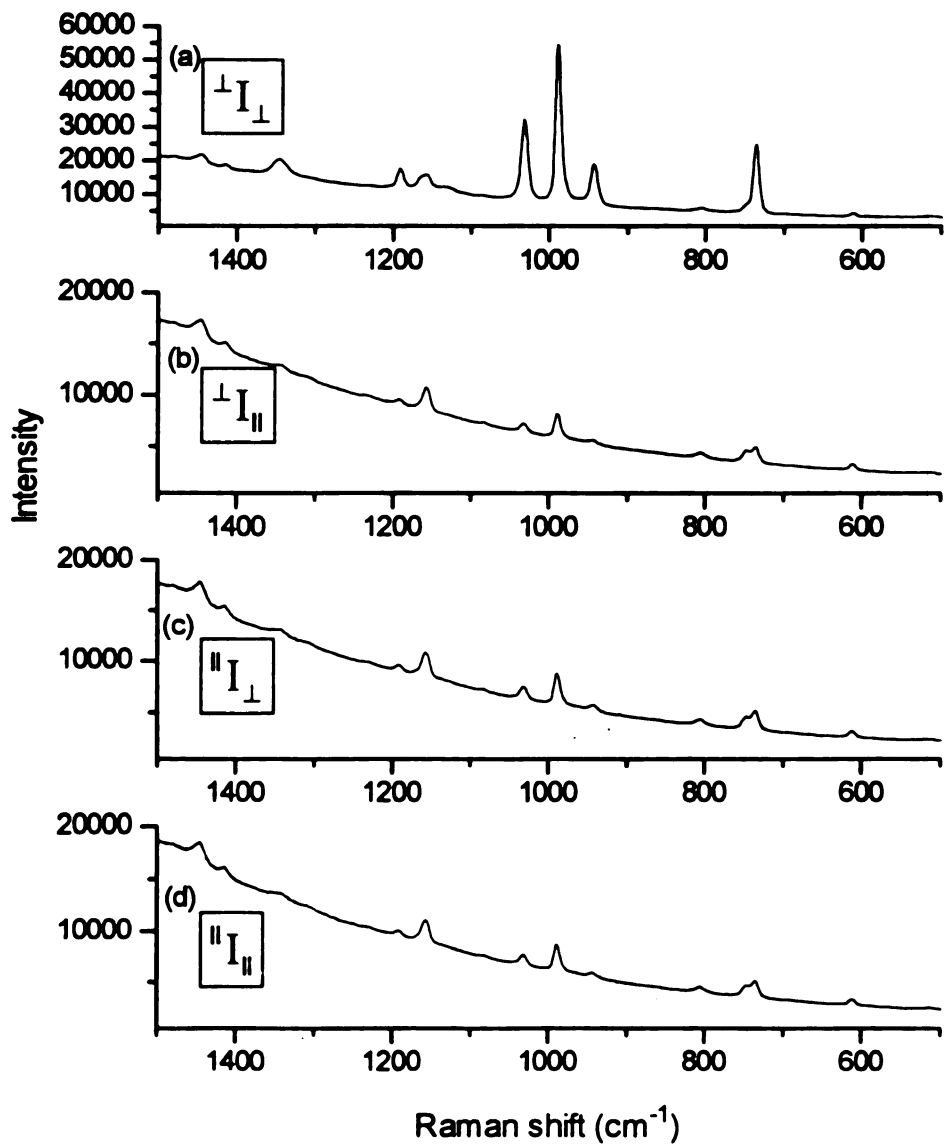


Figure 7. Raman spectra taken for different polarizations of N-N-dimethylaniline. (a)  $\perp I_{\perp}$ , (b)  $\perp I_{\parallel}$ , (c)  $\parallel I_{\perp}$ , (d)  $\parallel I_{\parallel}$ .

**Table 2.** The experimentally obtained intensity, cross-sectional area, calculated depolarization ratio,  $(\bar{\alpha}')$ <sub>i</sub>, and  $(\gamma')$ <sub>i</sub> of chlorobenzene for different modes.

Mode (cm <sup>-1</sup> )	<sup>1</sup> I <sub>1</sub>			<sup>1</sup> I <sub>u</sub>			<sup>3</sup> I <sub>1</sub>			<sup>3</sup> I <sub>u</sub>		
	1	2	3	1	2	3	1	2	3	1	2	3
1093	9770	30203	125418	801	2649	13312	1493	3262	12242	1119	3049	12866
1023	9383	27900	78351	860	1108	4978	649	1478	6594	321	1537	5820
1000	25319	81919	373748	891	3270	19124	1481	4441	15971	1279	4586	21357
638	6190	21343	81631	331	1162	6570	539	1601	5810	369	1149	6053
340	532	21711	91813	588	4217	19332	882	5750	18635	568	3817	18386

Table 2. (cont'd)

Mode (cm <sup>-1</sup> )	Cross-section (x10 <sup>-30</sup> cm <sup>2</sup> .molecule <sup>-1</sup> .Sr <sup>-1</sup> )	Average cross-section (x10 <sup>-30</sup> cm <sup>2</sup> .molecule <sup>-1</sup> .Sr <sup>-1</sup> )			Depolarization Ratio $\rho$	Average Depolarization Ratio $\bar{\rho}$
		1	2	3		
1093	5.16	4.97	5.29	5.14	0.247	0.192
1023	4.93	4.62	4.62	4.72	0.0946	0.104
1000	14.7	15.0	15.2	15.0	0.105	0.106
638	3.94	3.99	3.93	3.95	0.139	0.122
340	3.23	3.34	4.45	3.67	0.245	0.369
						0.333
						0.316

Table 2. (cont'd)

Mode (cm <sup>-1</sup> )	$(\bar{\alpha}'), (\times 10^{-5} \text{ cm}^2 \cdot \text{g}^{-1/2})$	$(r'), (\times 10^{-5} \text{ cm}^2 \cdot \text{g}^{-1/2})$
1093	3.640	5.203
1023	2.015	2.020
1000	3.562	3.321
638	1.363	1.474
340	1.648	3.192

**Table 3.** The experimentally obtained intensity, cross-sectional area, calculated depolarization ratio,  $(\bar{\alpha}')$ <sub>i</sub>, and  $(\gamma')$ <sub>i</sub> of bromobenzene for different modes.

Mode (cm <sup>-1</sup> )	${}^1I_1$			${}^1I_{11}$			${}^1I_{11}$		
	1	2	3	1	2	3	1	2	3
1077	15712	53952	71493	2305	4821	8141	3707	5111	13056
1021	21273	36956	78270	2887	3839	4538	4574	5402	10849
998	67335	220964	391753	8255	11071	27025	13471	16661	48660
603	16821	45033	74503	1601	1415	4602	3008	4098	8873
258	37465	84790	118708	9002	14113	24305	12944	21257	35664

\*Note: The values from the third experiment are omitted due to experimental errors.

Table 3. (cont'd)

Mode (cm <sup>-1</sup> )	Cross-section (x10 <sup>-30</sup> cm <sup>2</sup> .molecule <sup>-1</sup> .Sr <sup>-1</sup> )			Average cross-section (x10 <sup>-30</sup> cm <sup>2</sup> .molecule <sup>-1</sup> .Sr <sup>-1</sup> )	Depolarization Ratio $\rho$	Average Depolarization Ratio $\bar{\rho}$	
	1	2	3		1	2	3
1077	3.56	3.41	3.61	3.53	0.354	0.160	0.283
1021	5.69	5.37	5.38	5.48	0.301	0.261	0.193
998	16.9	15.4	15.4	15.9	0.295	0.135	0.199
603	3.53	3.53	3.60	3.55	0.272	0.134	0.183
258	4.18	4.24	7.08	5.17	0.505	0.379	0.438

\*Note: The values from the third experiment are omitted due to experimental errors.

Table 3. (cont'd)

Mode (cm <sup>-1</sup> )	( $\bar{\alpha}'$ ), (x10 <sup>-5</sup> cm <sup>2</sup> .g <sup>-1/2</sup> )	( $\gamma'$ ), (x10 <sup>-5</sup> cm <sup>2</sup> .g <sup>-1/2</sup> )
1077	1.602	2.658
1021	1.905	3.375
998	3.320	4.871
603	1.149	1.623
258	.6499	1.699

**Table 4.** The experimentally obtained intensity, cross-sectional area, calculated depolarization ratio,  $(\bar{\alpha}')$ <sub>i</sub>, and  $(\gamma')$ <sub>i</sub> of iodobenzene for different modes.

Mode (cm <sup>-1</sup> )	<sup>1</sup> I <sub>1</sub>			<sup>1</sup> I <sub>u</sub>			<sup>2</sup> I <sub>1</sub>			<sup>2</sup> I <sub>u</sub>		
	1	2	3	1	2	3	1	2	3	1	2	3
1068	9550	18505	8352	934	2293	1066	1340	2959	1705	75	2723	1132
1015	88521	155419	61954	2967	5942	2452	4943	6963	5166	5574	5745	2935
995	137575	299390	115212	10098	14766	6183	13724	26292	11697	13686	19541	7944
583	42204	97129	42248	2025	2633	1263	3141	5018	2674	2768	3616	2558
225	103634	237619	80598	23949	44340	16531	28712	55120	18883	26351	47074	18405

**Table 4.** (cont'd)

Mode (cm <sup>-1</sup> )	Cross-section (x10 <sup>-30</sup> cm <sup>2</sup> .molecule <sup>-1</sup> .Sr <sup>-1</sup> )	Average cross-section (x10 <sup>-30</sup> cm <sup>2</sup> .molecule <sup>-1</sup> .Sr <sup>-1</sup> )	Depolarization Ratio $\rho$	Average Depolarization Ratio $\bar{\rho}$
	1	2	3	
1068	1.45	1.13	1.17	0.135
1015	9.10	8.78	8.63	0.147
995	18.9	19.8	20.0	0.186
583	5.44	6.07	6.17	0.134
225	7.73	7.67	10.5	0.432

Table 4. (cont'd)

<b>Mode (cm<sup>-1</sup>)</b>	<b>(<math>\bar{\alpha}'</math>), (x10<sup>-5</sup> cm<sup>2</sup>.g<sup>-1/2</sup>)</b>	<b>(<math>\gamma'</math>), (x10<sup>-5</sup> cm<sup>2</sup>.g<sup>-1/2</sup>)</b>
1068	0.8820	1.380
1015	2.399	2.421
995	3.456	4.269
583	1.385	1.371
225	0.7218	1.683

**Table 5.** The experimentally obtained intensity, cross-sectional area, calculated depolarization ratio,  $(\bar{\alpha}')$ <sub>i</sub>, and  $(\gamma')$ <sub>i</sub> of toluene for different modes.

Mode (cm <sup>-1</sup> )	<sup>1</sup> I <sub>1</sub>			<sup>1</sup> I <sub>u</sub>			<sup>1</sup> I <sub>1</sub>			<sup>1</sup> I <sub>u</sub>		
	1	2	3	1	2	3	1	2	3	1	2	3
1211	139410	163867	113194	6411	8211	6042	8745	10437	10615	8528	8490	7833
1031	118259	138044	95341	4937	6168	5116	5774	7889	8230	6162	6579	5988
1004	449193	518084	371646	14748	15651	13775	20573	22180	26446	19803	18263	19704
786	239313	271426	206781	9338	9891	9041	12703	16441	16201	13855	10929	11933
521	61021	68701	52938	19108	16556	14139	18598	19285	17290	18597	17575	15156

Table 5. (cont'd)

Mode (cm <sup>-1</sup> )	Cross-section (x10 <sup>-30</sup> cm <sup>2</sup> .molecule <sup>-1</sup> .Sr <sup>-1</sup> )	Average cross-section (x10 <sup>-30</sup> cm <sup>2</sup> .molecule <sup>-1</sup> .Sr <sup>-1</sup> )	Depolarization Ratio $\rho$			Average Depolarization Ratio $\bar{\rho}$		
			1	2	3			
1211	3.80	3.76	4.66	4.08	0.118	0.110	0.155	0.128
1031	3.74	3.40	3.15	3.43	0.0969	0.100	0.142	0.113
1004	14.1	14.9	15.1	14.7	0.0870	0.0758	0.120	0.0942
786	8.15	8.13	7.85	8.05	0.107	0.0973	0.130	0.111
521	1.80	1.87	2.14	1.94	0.464	0.432	0.484	0.460

Table 5. (cont'd)

Mode (cm <sup>-1</sup> )	( $\bar{\alpha}'$ ), (x10 <sup>-5</sup> cm <sup>2</sup> .g <sup>-1/2</sup> )	( $\gamma'$ ), (x10 <sup>-5</sup> cm <sup>2</sup> .g <sup>-1/2</sup> )
1211	2.156	2.287
1031	1.800	1.778
1004	3.691	3.288
786	2.331	2.286
521	0.7096	1.937

Table 6. The experimentally obtained intensity, cross-sectional area, calculated depolarization ratio,  $(\bar{\alpha}')$ <sub>i</sub>, and  $(\gamma')$ <sub>i</sub> of aniline for different modes.

Mode (cm <sup>-1</sup> )	<sup>1</sup> I <sub>1</sub>			<sup>1</sup> I <sub>u</sub>			<sup>3</sup> I <sub>1</sub>			<sup>3</sup> I <sub>u</sub>		
	1	2	3	1	2	3	1	2	3	1	2	3
1278	239070	275244	189309	13948	14810	25637	13531	17457	16657	15166	16028	14262
1027	251365	278001	204336	8274	7273	38162	9798	11749	14217	10364	9702	11028
996	625307	681703	546540	27729	30477	70343	32915	36598	41563	32971	32389	33834
814	227316	241150	186742	2640	4477	38760	8481	11706	14294	10602	7260	18925
530	63679	44310	51064	20877	16113	47535	21487	23381	20872	21252	17760	18492

Table 6. (cont'd)

Mode (cm <sup>-1</sup> )	Cross-section (x10 <sup>-30</sup> cm <sup>2</sup> .molecule <sup>-1</sup> .Sr <sup>-1</sup> )	Average cross-section (x10 <sup>-30</sup> cm <sup>2</sup> .molecule <sup>-1</sup> .Sr <sup>-1</sup> )	Depolarization Ratio $\rho$	Average Depolarization Ratio $\bar{\rho}$
	1	2	3	
1278	7.67	8.10	7.35	0.113
1027	8.06	8.18	7.93	0.0777
996	20.4	19.3	20.4	0.101
814	7.29	7.09	7.25	0.0830
530	2.04	1.30	1.98	0.505

Table 6. (cont'd)

Mode (cm <sup>-1</sup> )	( $\bar{\alpha}'$ ), (x10 <sup>-5</sup> cm <sup>2</sup> .g <sup>-1/2</sup> )	( $\gamma'$ ), (x10 <sup>-5</sup> cm <sup>2</sup> .g <sup>-1/2</sup> )
1278	5.956	6.276
1027	5.400	4.477
996	8.273	7.995
814	4.381	4.169
530	1.254	3.940

**Table 7.** The experimentally obtained intensity, cross-sectional area, calculated depolarization ratio,  $(\bar{\alpha}')_i$ , and  $(\gamma')_i$  of N-N-dimethylaniline for different modes.

Mode (cm <sup>-1</sup> )	<sup>1</sup> I <sub>1</sub>		<sup>1</sup> I <sub>II</sub>		<sup>11</sup> I <sub>1</sub>		<sup>11</sup> I <sub>II</sub>	
	1	2	1	2	1	2	1	2
1190	54742	82156	3724	9812	12770	9162	7657	12188
1031	155341	367479	6610	15402	13529	17773	8582	28692
988	244590	549573	13180	31127	30077	40846	16374	365558
735	98160	260743	11800	21601	51862	25618	12829	45142

Table 7. (cont'd)

Mode (cm <sup>-1</sup> )	Cross-section (x10 <sup>-30</sup> cm <sup>2</sup> .molecule <sup>-1</sup> .Sr <sup>-1</sup> )		Average cross-section (x10 <sup>-30</sup> cm <sup>2</sup> .molecule <sup>-1</sup> .Sr <sup>-1</sup> )	Depolarization Ratio $\rho$	Average Depolarization Ratio $\bar{\rho}$
	1	2		1	
1190	2.15	1.44	1.79	0.349	0.232
1031	6.10	6.42	6.26	0.137	0.121
988	6.67	12.5	9.61	0.180	0.133
735	3.85	4.56	4.21	0.588	0.251
					0.419

**Table 7.** (cont'd)

<b>Mode (cm<sup>-1</sup>)</b>	<b>(<math>\bar{\alpha}'</math>), (x10<sup>-5</sup> cm<sup>2</sup>.g<sup>-1/2</sup>)</b>	<b>(<math>\gamma'</math>), (x10<sup>-5</sup> cm<sup>2</sup>.g<sup>-1/2</sup>)</b>
1190	2.393	4.346
1031	7.850	8.375
988	5.278	6.331
735	2.480	6.155

Figures 8 to 27 show the graphs of  $(\bar{\alpha}')$  and  $(\gamma')$  plotted with respect to the hyperpolarizability,  $\beta$ . The values of the hyperpolarizability,  $\beta$ , in figures 8 to 17 are taken from ref. 16 whereas in figures 18 to 27 the values are taken from ref. 17. The one main difference between these two references is that in ref. 16 the value of aniline is tabulated and in ref. 17 the value of N-N-dimethylaniline is tabulated.

### 3.3. Conclusion

Data in their current form show a definite correlation between the Raman intensities and the  $\beta$  hyperpolarizabilities of the species and vibrations studied.

There are strong correlations between  $\beta$  and the derivative of the isotropically averaged polarizability with respect to vibrational mode #2 in this work, based on either set of data for the  $\beta$  hyperpolarizabilities. R values for the straight line fits are  $\sim 0.97$  in one case and  $\sim 0.96$  in the other. A relatively high level of correlation between  $(\bar{\alpha}')$ , and  $\beta$  is observed for  $\beta$  values from the first set of literature data, and vibrational modes  $i = 1$  to 4 (R ranges from  $\sim 0.87$  to  $\sim 0.97$ ), and moderate correlations are found for  $(\gamma')$ , and  $\beta$ ,  $i = 1$  to 5 (R ranges from  $\sim 0.68$  to  $\sim 0.88$ ). Generally, correlations are weaker based on the second set of  $\beta$  values from the literature, although even in this case, for particular modes and particular choice of isotropic vs. depolarized Raman scattering, high R values can be found (R  $\sim 0.96$  and 0.92 in two cases).

To determine the validity of the correlations and to determine whether differences in R values between modes and between  $\alpha$  and  $\gamma$  derivatives are chemically meaningful, it will be necessary to obtain highly reliable data on the Raman intensities and to discriminate among literature values of  $\beta$ .

**Figure 8.** Graph of  $(\bar{\alpha}')_1$  vs.  $\beta$ .

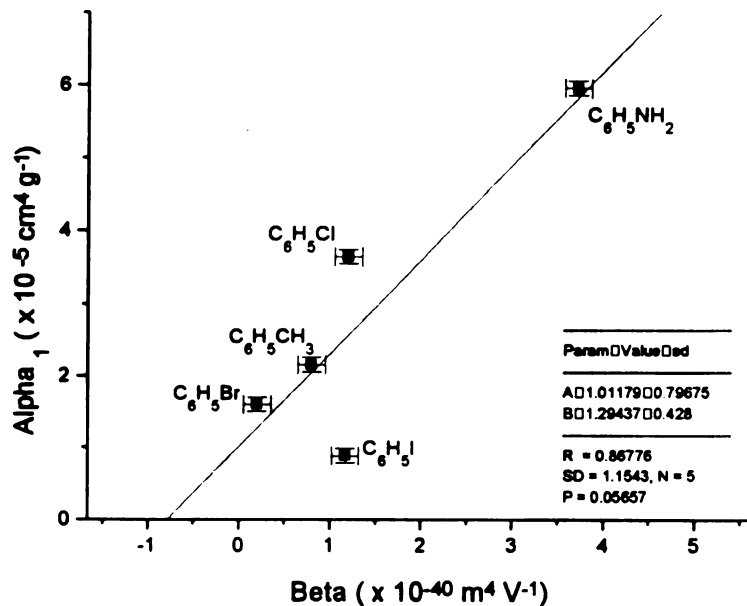


**Figure 9.** Graph of  $(\bar{\alpha}')_2$  vs.  $\beta$ .

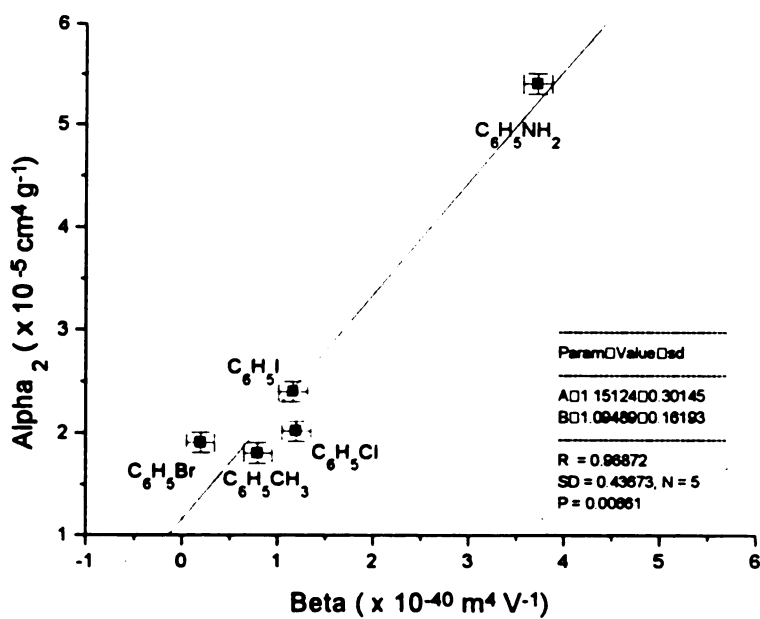


Figure 10. Graph of  $(\bar{\alpha}')$ <sub>3</sub> vs.  $\beta$ .

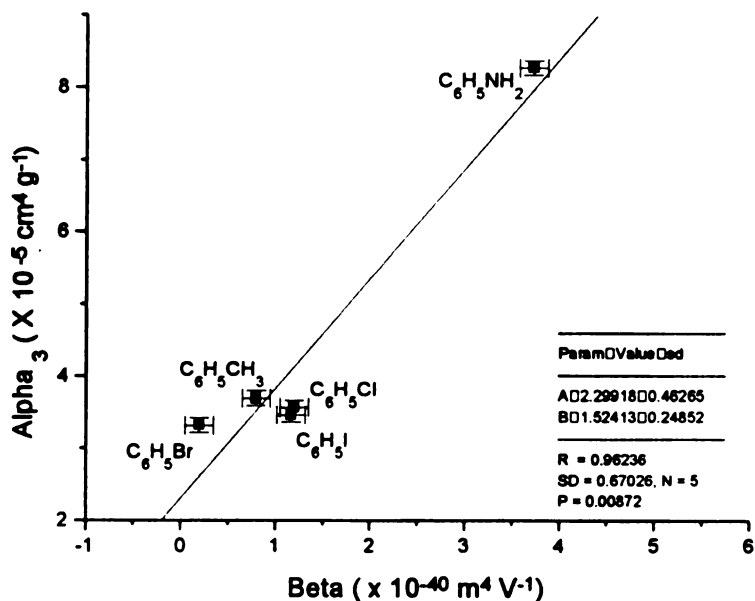
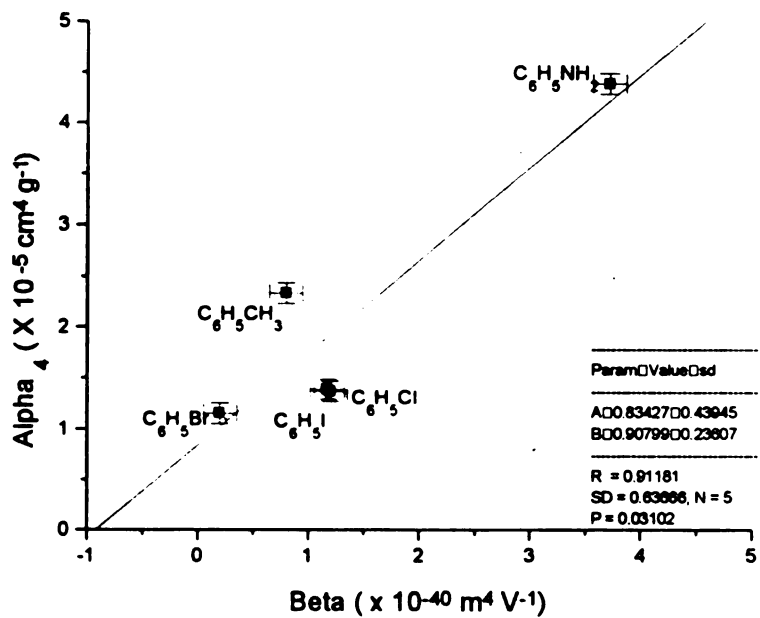
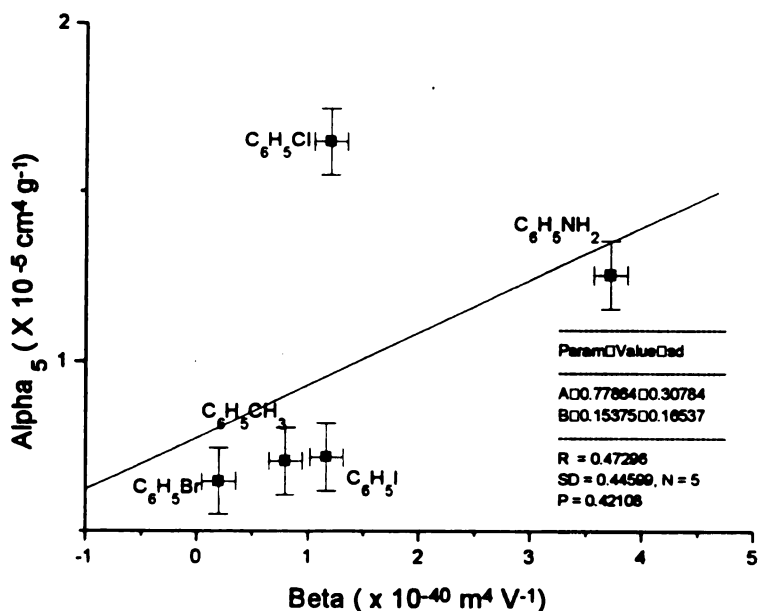


Figure 11. Graph of  $(\bar{\alpha}')$ <sub>4</sub> vs.  $\beta$ .



**Figure 12.** Graph of  $(\bar{\alpha}')_s$  vs.  $\beta$ .



**Figure 13.** Graph of  $(\gamma')_1$  vs.  $\beta$ .

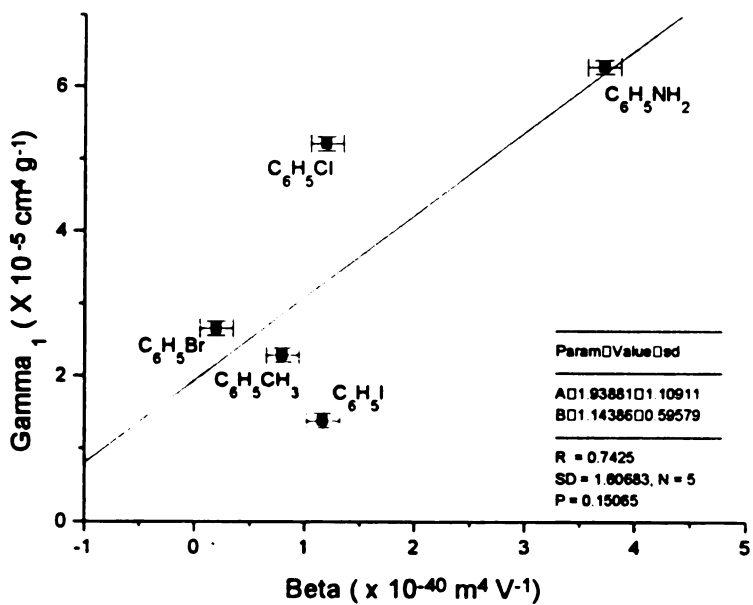


Figure 14. Graph of  $(\gamma')_2$  vs.  $\beta$ .

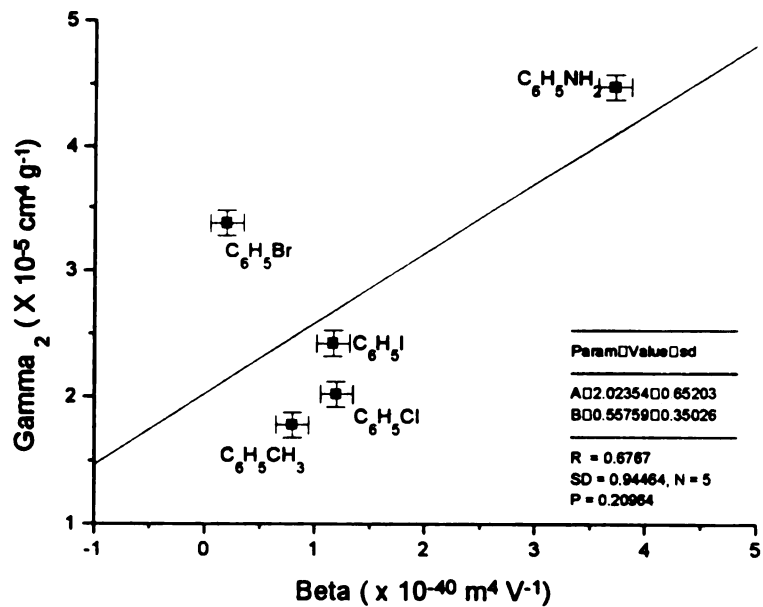


Figure 15. Graph of  $(\gamma')_3$  vs.  $\beta$ .

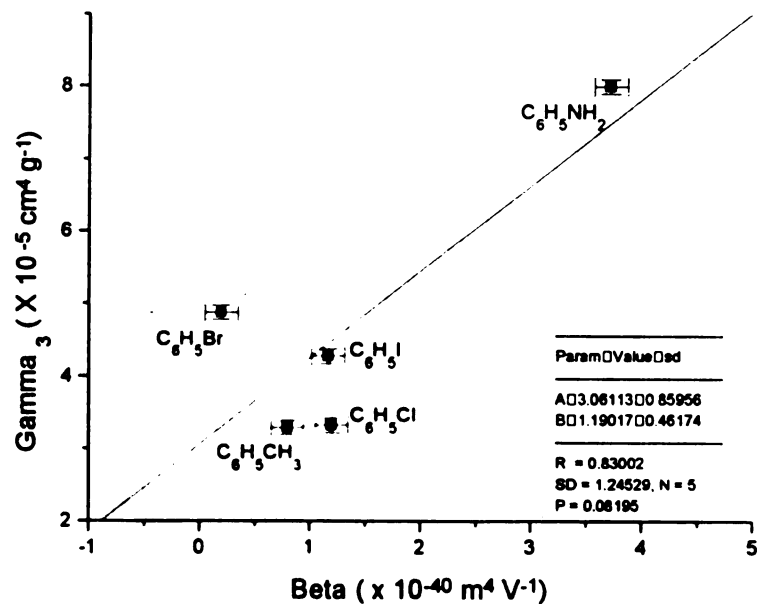


Figure 16. Graph of  $(\gamma')_4$  vs.  $\beta$ .

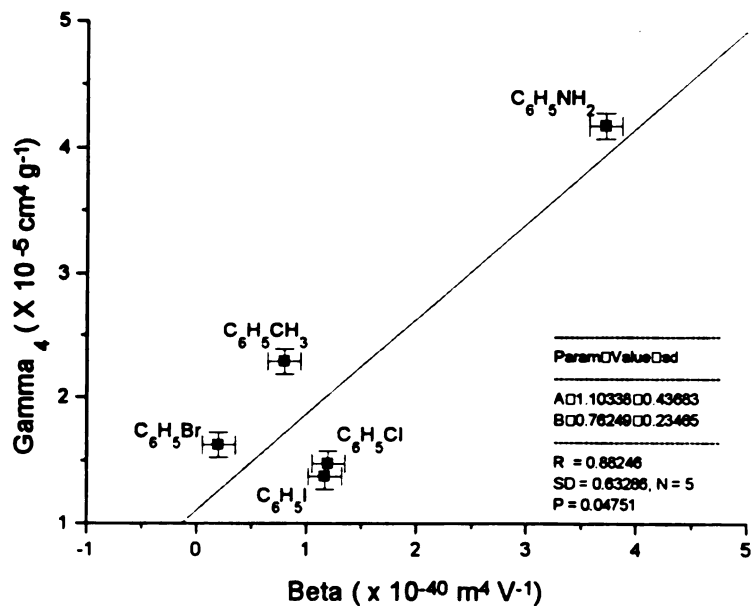


Figure 17. Graph of  $(\gamma')_5$  vs.  $\beta$ .

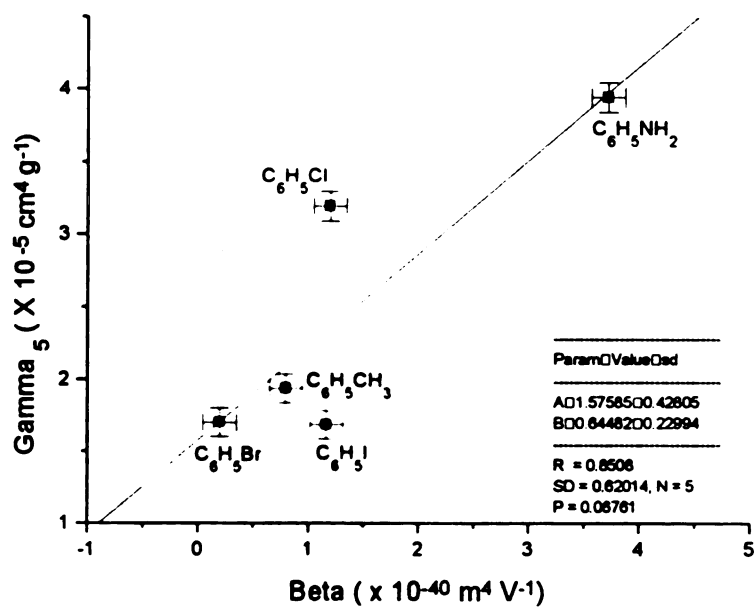


Figure 18. Graph of  $(\bar{\alpha}')_1$  vs.  $\beta$ .

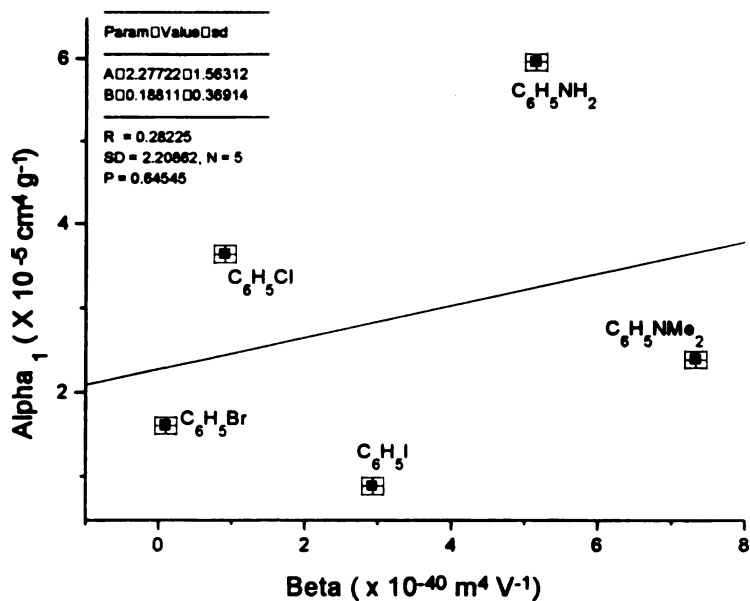
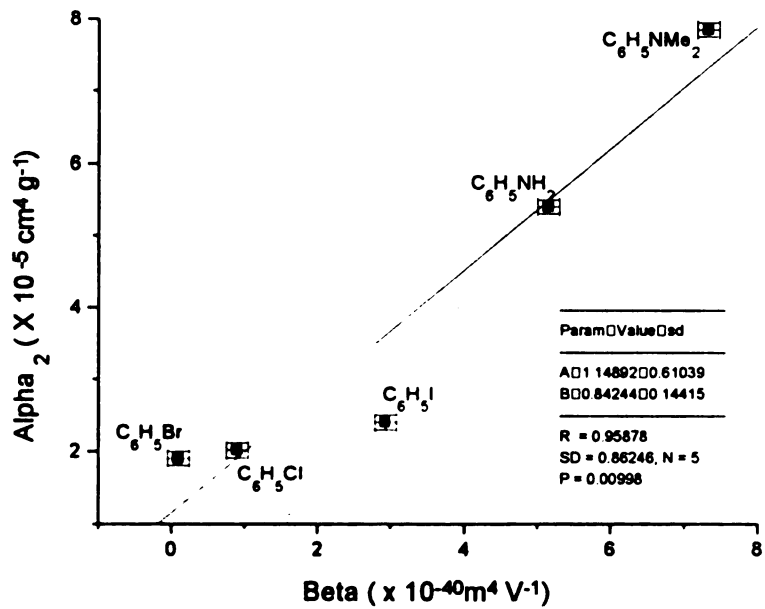
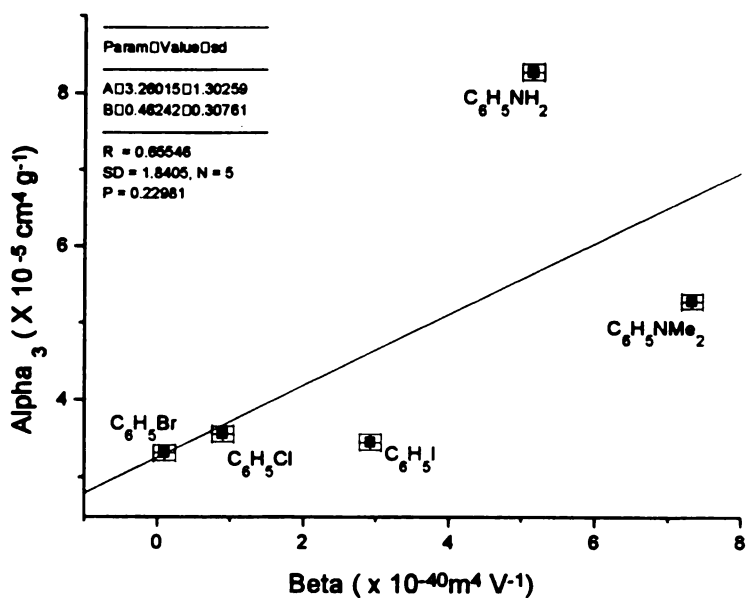


Figure 19. Graph of  $(\bar{\alpha}')_2$  vs.  $\beta$ .



**Figure 20.** Graph of  $(\bar{\alpha}')$ <sub>3</sub> vs.  $\beta$ .



**Figure 21.** Graph of  $(\bar{\alpha}')$ <sub>4</sub> vs.  $\beta$ .

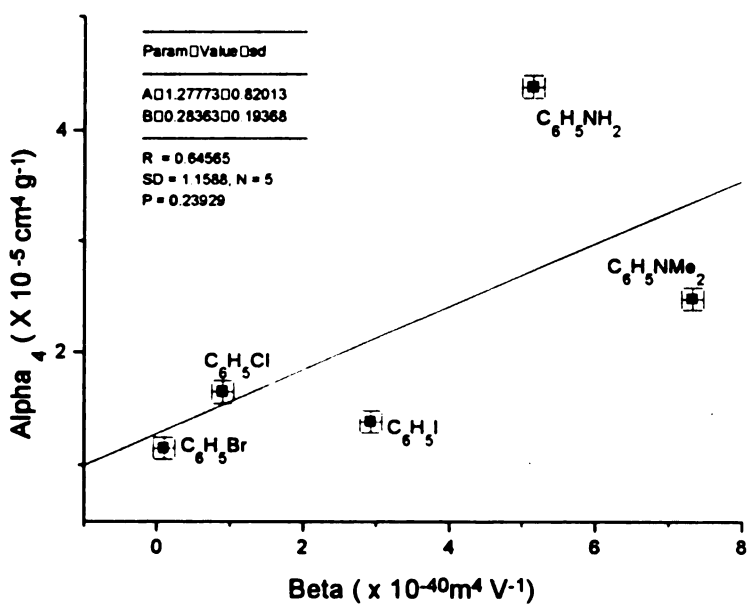


**Figure 22.** Graph of  $(\bar{\alpha}')_s$  vs.  $\beta$ .

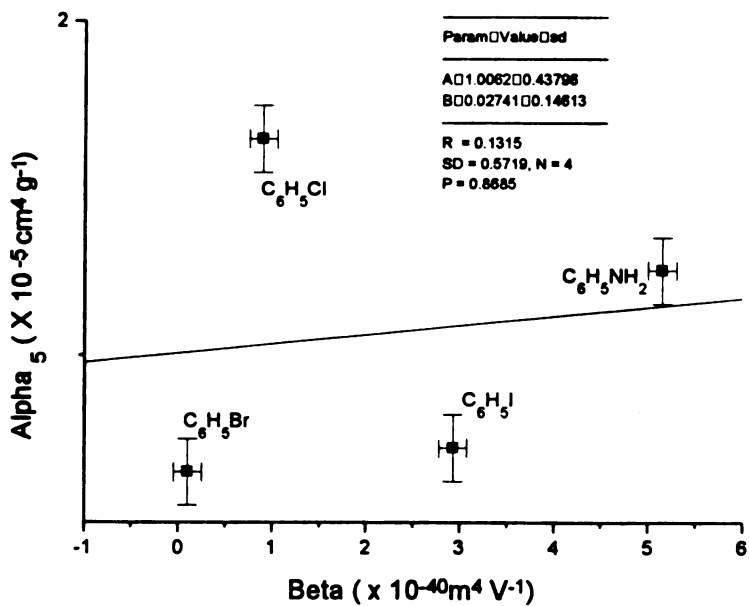


**Figure 23.** Graph of  $(\gamma')_1$  vs.  $\beta$ .

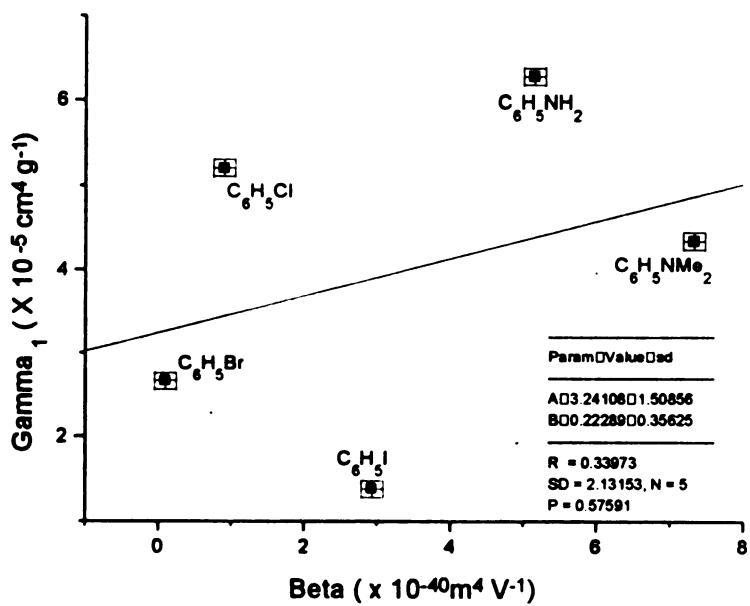


Figure 24. Graph of  $(\gamma')_2$  vs.  $\beta$ .

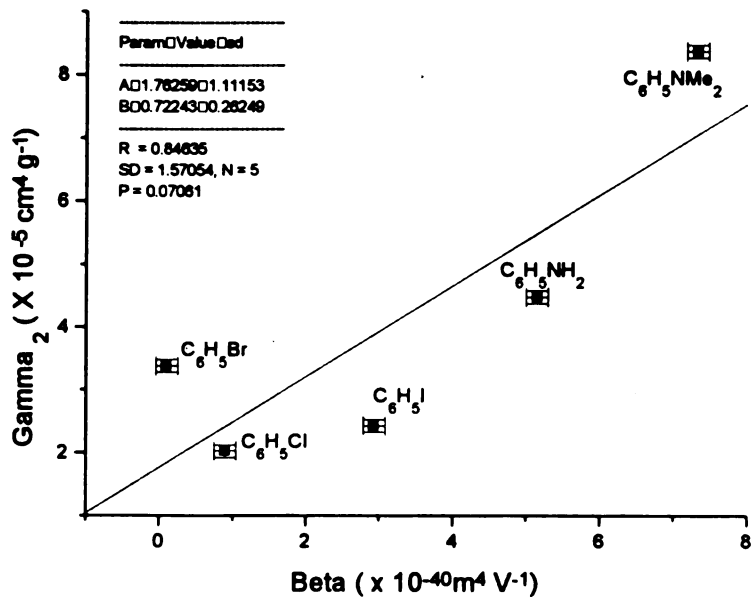


Figure 25. Graph of  $(\gamma')_3$  vs.  $\beta$ .

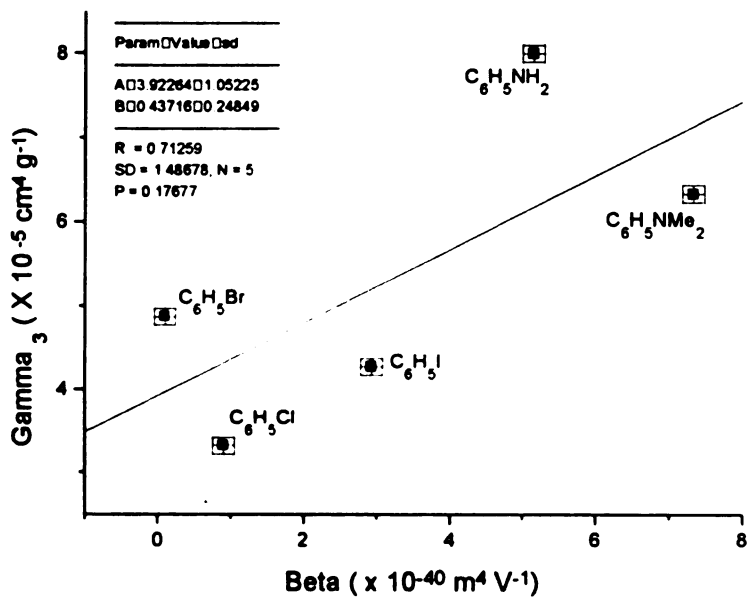


Figure 26. Graph of  $(\gamma')_4$  vs.  $\beta$ .

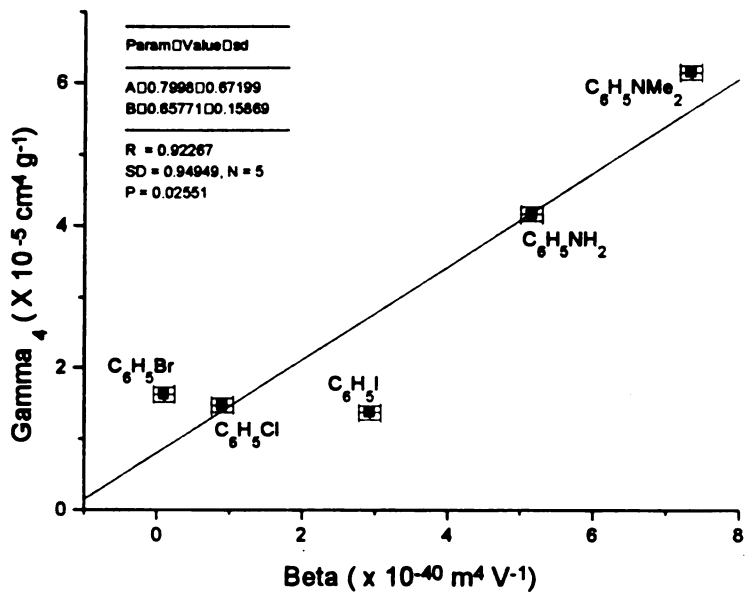
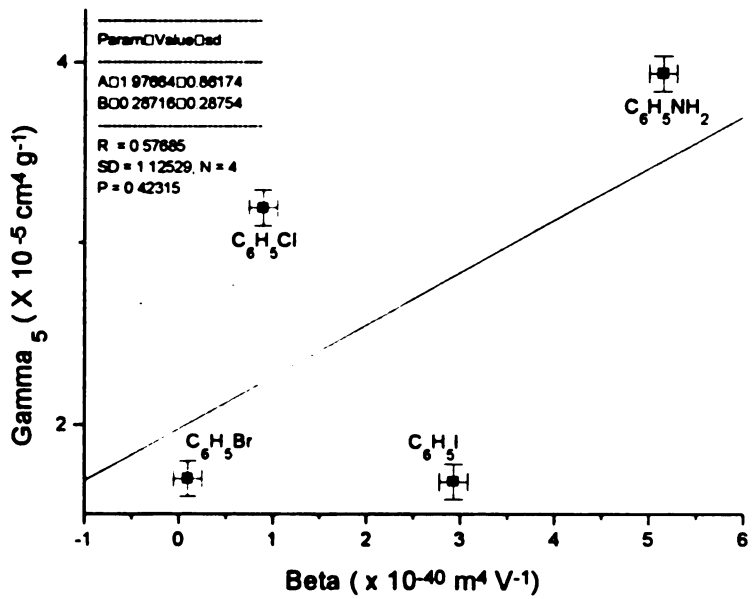


Figure 27. Graph of  $(\gamma')_5$  vs.  $\beta$ .



### 3.4. References

1. J. Behringer, *Raman Spectroscopy*, H. A. Szymanski, Ed. (Plenum, New York, 1967), p. 168.
2. P. P. Shorygin and T. M. Ivanova, *Opt. Spektrosk.* **25**, 200 (1968) [Opt. Spectrosc. **25**, 107 (1968)].
3. J. H. Van Vleck, *Proc. Natl. Acad. Sci. (U.S.)* **15**, 754, (1929).
4. G. Placzek, *Handbuch der Radiologie*, edited by E. Marx (Akademische Verlagsgesellschaft, Leipzig, 1934), Vol. 6, Chap. 2, p. 205.
5. A. C. Albrecht, *J. Chem. Phys.* **34**, 1476 (1961).
6. L. Petricolas, L. Nafie, P. Stein, and B. Fanconi, *J. Chem. Phys.* **52**, 1576 (1970).
7. F. A. Savin and I. I. Sobel'man, *Opt. Spektrosk.* **7**, 733 (1959) [Opt. Spectrosc. **7**, 435 (1959)].
8. E. A. Power and S. Zienau, *Phil. Trans. Roy. Soc. (London)* **A251**, 427 (1959).
9. J. Fiutak, *Can. J. Phys.* **41**, 12 (1963).
10. Y. Kato and H. Takuma, *J. Opt. Soc. Am.* **61**, 347 (1971).
11. Y. Kato and H. Takuma, *J. Chem. Phys.* **54**, 5398 (1971).
12. J. A. Armstrong, N. Bloembergen, J. Ducuing, and P. S. Pershan, *Phys. Rev.* **127**, 1918 (1962).
13. G. Eckhardt and W. G. Wagner, *J. Mol. Spectry.* **19**, 407 (1966).
14. D. A. Long, *Raman Spectroscopy* (McGraw-Hill, Great Britain, 1977) p. 59.
15. Microcal Software, Inc., *The Peak Fitting Module Manual*, p. 41.
16. B. F. Levine and C. G. Bethea, *J. Chem. Phys.* **63**, 2666 (1975).
17. J. L. Oudar and H. Le Person, *Opt. Commun.* **15**, 258 (1975).

## **Chapter 4**

### **Future Work**

#### **4.1. Extension of These Experiments**

In our earlier experiments, we have obtained ( $\overrightarrow{\alpha}'$ ) and ( $\gamma'$ ) for 5 modes of six monosubstituted benzene molecules. However, to test more adequately for a correlation between Raman intensities and hyperpolarizabilities, additional data are required.

We have propose to continue this experiment using other species with known  $\beta$  values that can also be easily handled in the lab.

Calculations on two particular molecules (bromobenzene and N-N-dimethylaniline) from the earlier experiments need to be redone. The data from bromobenzene did not give a satisfactory result; and N-N-dimethylaniline fluoresced during the experiment making it difficult to obtain a 'clean' spectra. What we have proposed is to use the Ti-Sapphire laser to obtain a better spectra in the case of N-N-dimethylaniline.

#### **4.2. Computational Calculation on the Hyperpolarizability Density in a Non-uniform Field Environment**

In the 1960s, Lipscomb *et al.*<sup>1-5</sup> proposed a set of computational calculation on molecular properties based upon a perturbed Hartree-Fock calculations. Lipscomb *et al.* solved the limited basis set Hartree-Fock problem in the presence of a perturbation term in the Hamiltonian to obtain the first-order perturbed wavefunction, in a uniform field. They then applied the formulation to the calculation of electric polarizability, magnetic susceptibility, and magnetic shielding all in an invariant and uniform electric field environment.

What we propose to do is to compute the exact kind of calculation but in a non-uniform electric field environment.

**4.3. References**

1. R. M. Stevens, R. M. Pitzer, and W. N. Lipscomb, *J. Chem. Phys.* **38**, 550 (1963).
2. R. M. Stevens and W. N. Lipscomb, *J. Chem. Phys.* **40**, 2238 (1964).
3. R. M. Stevens and W. N. Lipscomb, *J. Chem. Phys.* **41**, 184 (1964).
4. R. M. Stevens and W. N. Lipscomb, *J. Chem. Phys.* **41**, 3710 (1964).
5. R. M. Stevens and W. N. Lipscomb, *J. Chem. Phys.* **42**, 3666 (1965).

MICHIGAN STATE UNIV. LIBRARIES



31293013992296